APPLICATION OF PREDICTIVE COMBUSTION MODEL TO CI ICE BASED ON LES AND CHEMICAL KINETICS

OLDŘICH VÍTEK, VÍT DOLEČEK, MARCEL DIVIŠ, JAN MACEK

Czech Technical University in Prague, Department of Automotive, Combustion Engine and Railway Engineering, Technická 4, CZ-16607 Prague 6, Czech Republic, Tel.: +420224352507, Fax: +420224352500
E-mail: oldrich.vitek@fs.cvut.cz, marcel.skarohlid@fs.cvut.cz, jan.macek@fs.cvut.cz

ABSTRACT

The paper deals with 3-D CFD modeling of CI ICE while using LES approach combined with chemical kinetics. Detailed CFD model of single-cylinder research CI engine was built. As LES approach has high predictive ability, it needs limited calibration when compared with RANS. In this particular case, only LES spray sub-model was calibrated using dedicated data from 'cold' pressure vessel test rig. Another critical step when using LES approach is to have a correct computational mesh resolution. Global heat transfer scaling factor was fine-tuned as well. Sensitivity studies were carried out to make the final selection of these parameters. After that, 4 different engine operating points were calculated – these represent different load levels while there is a variation of EGR as well. Concerning applied chemistry, simple mechanism based on n-heptane containing 34 species and 64 reactions was used. Predicted data were compared versus measured/reference data representing average cycle. Good performance of applied simulation setup was stated – this mainly concerns the predictive ability in terms of rate of heat release and NO_x formation. Certain shortcomings were identified – they need addressing, which is planned as near-future steps.
KEYWORDS: LES, CFD, CHEMICAL KINETICS, COMPRESSION IGNITION, SIMULATION, NO_x FORMATION, IGNITION DELAY

SHRNUTÍ

Článek se zabývá 3-D CFD modelováním vznětového spalovacího motoru za použití LES přístupu v kombinaci s chemickou kinetikou. Byl vytvořen podrobný CFD model jednoválcového výzkumného vznětového motoru. Protože LES přístup vykazuje velkou prediktivní schopnost, nutnost kalibrace je nižší ve srovnání s RANS přístupem. V tomto konkrétním případě jen LES model paprsku paliva byl kalibrován s využitím dat ze „studené" tlakové komory. Dalším kritickým krokem při použití LES je použití správné výpočetní sítě z hlediska jejího rozlišení. Také globální násobitel pro přestup tepla byl mírně doladěn. Pro finální výběr těchto parametrů byly provedeny citlivostní studie. Poté byly propočteny 4 různé pracovní body motoru – ty reprezentují různé úrovně zatížení s tím, že se mění i hodnota vnější recirkulace výfukových plynů. Co se týká použité chemie, byl použit jednoduchý mechanismus založený na n-heptanu, který obsahuje 34 složek a 64 reakcí. Vypočtená data byla porovnána s experimentálními/referenčními daty, která odpovídají průměrnému cyklu. Bylo konstatováno, že použitá konfigurace výpočtu vykazuje dobré parametry – to se týká hlavně schopnosti predikovat rychlost vývinu tepla a tvorbu NO_x. Byly identifikovány určité nedostatky, které je nutné řešit, což je plánováno pro nejbližší budoucnost.
KLÍČOVÁ SLOVA: LES, CFD, CHEMICKÁ KINETIKA, VZNĚCOVÁNÍ, SIMULACE, TVORBA NO_x, PRŮTAH VZNĚTU

1. INTRODUCTION

The future of CI ICE engines might not be that optimistic at the moment (mainly due to the 'diesel-gate' affair), however if CO_2 targets are to be fulfilled, it will be more difficult to achieve that without CI ICEs as their high thermal efficiency is unrivalled. This concerns automotive sector mainly. When dealing with power generation sector, there is already a strong competition from lean-burn gas SI ICEs. Regarding ship propelling, the position of CI ICEs is very strong. Hence, CI ICEs are very important in different industry sectors and it is needed to continue their development to improve BSFC and minimize pollutant formation.

The large-eddy simulation (LES) approach has become very popular recently as it offers significantly improved modelling of turbulence when compared with 'classical' RANS approach.

However, this comes with high price as LES calculations are very time demanding. Moreover, they usually require multi-cycle calculations and their subsequent statistical analysis, which makes them even more demanding. These factors lead to a fact that LES is mainly applied in academic/scientific projects. However, LES has been becoming more popular in industry sector recently as well.

Most of LES-focused papers are related to SI ICEs due to the fact that these engines feature high cycle-to-cycle variability (CCV), which can be correctly predicted by LES approach. Moreover, SI ICE combustion is very sensitive to local thermodynamic properties, which are strongly influenced by turbulence (mixing/diffusion, flame front propagation, interaction between spray and gas phase, etc.) while combustion process is relatively simple from chemical point of view (e.g., low concentration gradients, high local temperatures). These effects are captured properly by LES – c.f. [1, 2, 3, 4, 5, 6, 7, 8].

Surprisingly low amount of LES work is dedicated to CI ICEs while a lot of that is focused on sprays only – c.f. [9, 10, 11, 12, 13, 14]. This is mainly related to the fact that these engines have very low CCV. Although turbulence modeling is also important when dealing with simulation of CI ICEs, local chemical effects need to be captured properly as turbulence-chemistry interaction is a critical factor. Interaction between high-pressure fuel jet with gaseous phase is of primarily importance – this requires very fine mesh resolution. Moreover, combustion process is more complex when compared with SI ICE. All these phenomena contribute to the fact that LES is less popular in the domain of CI ICE combustion modeling. However, the authors are convinced that improved turbulence modeling by LES approach has high potential to improve CI ICE simulations. Hence, the LES approach is adopted in the presented paper.

It is well-known that chemistry of CI CIE combustion is relatively complex due to high variation of local air-to-fuel ratio and temperature. These effects are difficult to be modeled correctly as it requires solution of detailed chemistry based on chemical kinetics. Hence, simplified models are usually applied within RANS framework. However, these models require a lot of user tuning to match experimental data as their predictive ability is low. As the paper is focused on predictive combustion modeling, chemical kinetics was selected to simulate combustion process in CI ICE.

Based on above mentioned, the following goals were considered when dealing with detailed CFD modeling of CI ICE combustion:

- To apply LES 3-D CFD approach combined with chemical kinetics for the case of research single-cylinder CI internal combustion engine (ICE).

- To considered different operating conditions in terms of both BMEP and EGR.
- To compare predicted data with measured one including the analysis of differences between them.
- To perform sensitivity studies of selected parameters of CFD model setup.

2. MATHEMATICAL MODEL

For the simulation of the gas flow, spray mixture formation and combustion processes in the CI-engine analyzed in the present work, the 3D-CFD code AVL FIRE is adopted [36]. The 3-D CFD SW solves the general conservation equations of mass, momentum and enthalpy plus additional transport equations for turbulence related quantities and for conservation of chemical species. Depending on the physical and chemical sub-models employed, additional scalar quantities, such as e.g. mixture fraction, reaction progress variable, etc. are solved as well.

The adopted solution method is based on a fully conservative finite volume approach. All dependent variables, such as momentum, pressure, density, turbulence kinetic energy, dissipation rate, and the scalar quantities are evaluated at the cell centers of the general, unstructured computational grids. A second-order midpoint rule is used for integral approximation and a second order linear approximation for any value at the cell-face. Convection is solved by adopting higher order differencing schemes. In order to offer full flexibility in terms of the structure and topology of the employed computational meshes, the solver allows for each computational cell to consist of an arbitrary number of cell faces. Connectivity and interpolation practices for gradients and cell-face values are set up to accommodate such 'polyhedral' calculation volumes. The rate of change (accumulation term) is discretized by using an Euler implicit scheme. The overall solution procedure is iterative and is based on the Pressure-Implicit with Splitting of Operators (PISO, c.f. [15]), applicable to turbulent flows at all speeds. For solving the large sets of linear equation systems evolving from the discretization of the governing equations, an efficient preconditioned conjugate gradient method is employed. More details can be found in [1, 2] and documentation of AVL FIRE [36].

Dealing with numerical setup, the following settings were applied. PISO algorithm was selected as time integration method while 2nd order schemes were used for convective term approximations. Time step was set to 0.1 degCA with the exception of combustion phase when 0.005 degCA to capture interaction of spray with the smallest turbulence eddies.

Regarding turbulence modelling, Large Eddy Simulation (LES) was adopted. It is based on the filtered instantaneous Navier-Stokes equations. Filtering operation actually represents scale

separation in space, where large scales are directly resolved and the influence of small scales is taken into account by the sub-grid scale (SGS) model. Coherent structure version of LES approach [16, 18, 19] was selected for the considered engine case. The LES approach proved to be very effective for SI ICE cases (c.f. [1, 2, 3]), hence it was applied in the presented work as well.

Concerning combustion model, detailed chemistry solution was adopted by means of chemical kinetics application. Each computational cell is treated as single zone 0-D homogeneous reactor to calculate source terms for species transport equations and energy equation – this approach is based on [24]. These source terms are determined by means of solving equations of chemical kinetics for a selected reaction mechanism – in this particular case, relatively simple chemical mechanism based on n-heptane containing 34 species and 64 reactions was applied. It is known that the application of detailed chemical reactions in CFD can be quite time consuming. The 'chemistry clustering' model provides one way to reduce calculation times significantly. The background of the model is that in a large CFD domain, there are at every time step many cells which have similar thermodynamic conditions (temperature, equivalence ratio, etc.). These similar cells are identified and grouped to 'clusters'. The solution of the chemical reactions is only done for the mean of each cluster. After the results from the chemistry solver have been acquired, the species vector and the energy source have to be mapped back to the cells contained in the cluster. More details can be found in [26].

The spray model adopted in the present study is based on the Lagrangian Discrete Droplet Method (DDM) [21]. In the DDM the continuous gaseous phase is described by the standard Eulerian conservation equations, whereas the transport of the dispersed phase is calculated by tracking the trajectories of representative droplet parcels. A parcel consists of a number of droplets, with all the droplets having identical physical properties and behaving equally when they move, break up, hit a wall or evaporate. The calculation of the parcel movement is done with a sub-cycling procedure between the gas phase time steps taking into account the forces exerted on the parcels by the gas phase as well as the related heat and mass transfer. The coupling between the liquid and the gaseous phases is achieved by source term exchange for mass, momentum, energy and turbulence. For the LES application, turbulent dispersion effects are assumed to be fully covered by the interaction of the droplets with the resolved LES flow field scales – hence, this term is deactivated when LES approach is applied.

The CFD model is based on existing engine geometry (c.f. Table 1, Figure 1). 3-D CAD data of engine cylinder head, piston and liner were provided by engine manufacturer. All the necessary geometry information was available, hence the meshing procedure could be started. The meshing itself was made by means of hybrid meshing tool of AVL FIRE. Typical mesh cell size was set to 0.7 mm, however there is significant mesh refinemen along injection axes (especialy near injetor hole outlet). The important parameters of applied meshes are summarized in Table 2.
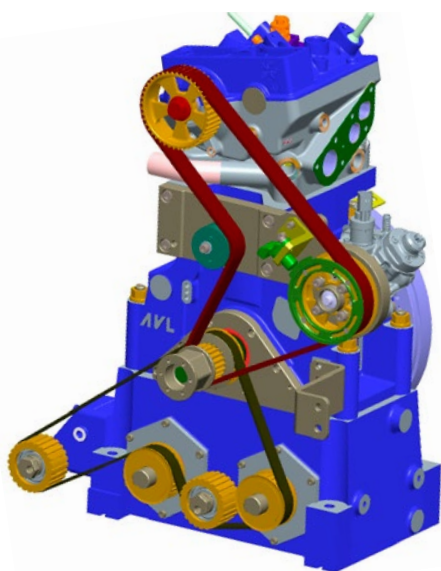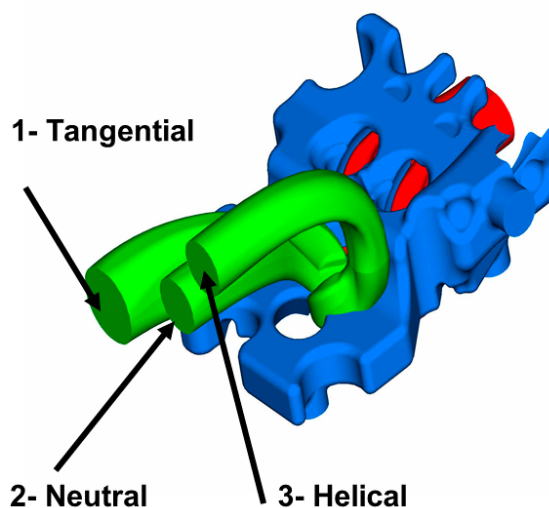

FIGURE 1: Target engine – AVL Single Cylinder Research Engine (CI version).
OBRÁZEK 1: Cílový motor – zkušební jednoválec od AVL (vznětová varianta).

Engine Parameter	Unit	Value
Bore-to-Stroke Ratio	[1]	0.944
Compression Ratio	[1]	15.9
Charging		Supercharged
Fuel		Diesel
Fuel Injection		Direct
Injection System		Common-rail
Number of Intake Valves		2
Number of Exhaust Valves		2

TABLE 2: Main mesh parameters of the considered engine case.
TABULKA 2: Hlavní parametry sítě pro uvažovaný motor.

Parameter	Unit	Value
Typical Mesh Size	[mm]	<0.7
Min. Amount of Mesh Cells	[1]	2.5M
Max. Amount of Mesh Cells	[1]	8.9M
Max. Angle Interval of Single Mesh Set	[degCA]	10

TABLE 3: Selected operating conditions of the engine.
TABULKA 3: Vybrané pracovní body motoru.

Engine Parameter	Unit	Case 1	Case 6	Case 15	Case 18
Engine Speed	[rpm]	1500	1500	1800	1800
BMEP	[bar]	17.0	7.6	14.1	7.7
Air Excess	[1]	1.25	2.9	1.2	2.4
EGR	[%]	0	0	21	19

Concerning boundary and initial conditions, they were transferred from the calibrated 0-D/1-D model of the engine created in SW tools [37]. Surface temperatures were based on simplified predictive FEM model, inlet/outlet boundary pressure/temperature was imposed as function of crank angle. The same applies to fuel mass-flow rate out of the injector based on calibrated injector model (which is contained in calibrated 0-D/1-D model of the target engine). Initial values of all required thermodynamic parameters (including composition) were directly transferred from the 0-D/1-D model.
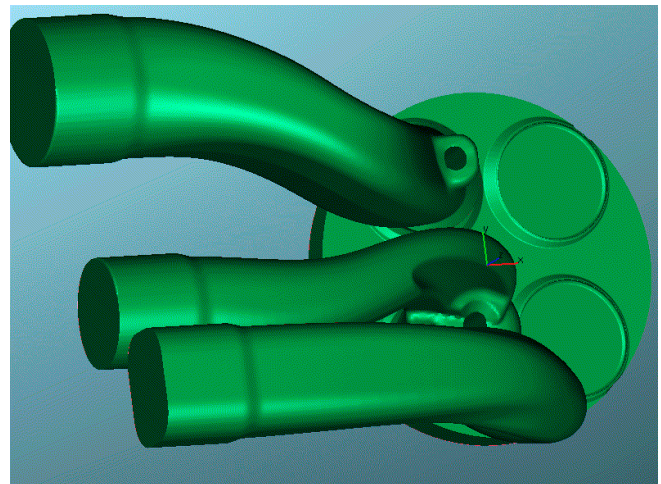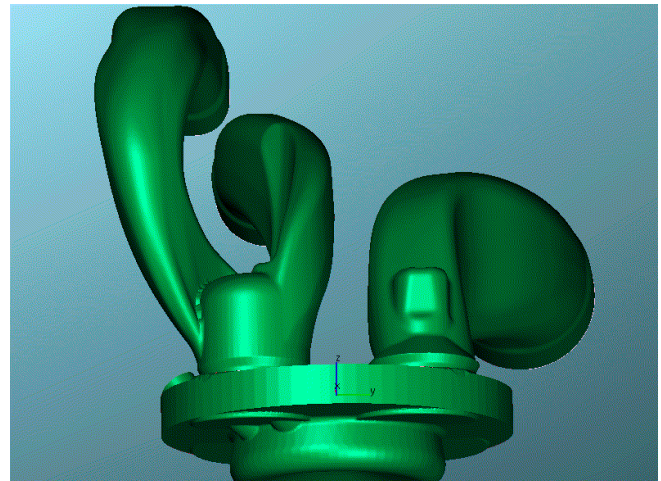

FIGURE 2: 3-D CAD geometries of considered engine case (Table 1 a 2).
OBRÁZEK 2: 3-D CAD geometrie uvažovaného motoru (tabulky 1 a 2).

3. COMPUTED CASES

The considered engine (c.f. Table 1 and 2, Figure 1 and 2) represents the research single cylinder CI engine from AVL. There are many experimental data available for this engine. For the presented study, the single-pilot fuel injection pattern was adopted while combustion timing was kept constant (to be more precise, CA50 was constant – angle location when 50% of the fuel is burnt was always the same) and while injection rail pressure was set to 150 MPa. The level of air excess (between 1.1 and 2.9 based on incoming fresh air) and EGR (between 0 and 22%) were varied while engine speed was kept between 1500 and 2000 rpm. Hence, different engine load levels were achieved (BMEP between 7 and 17 bar). Due to very time consuming 3-D CFD calculations, 4 operating points were selected covering high/lol BMEP at medium/low EGR level – these are summarized in Table 3.
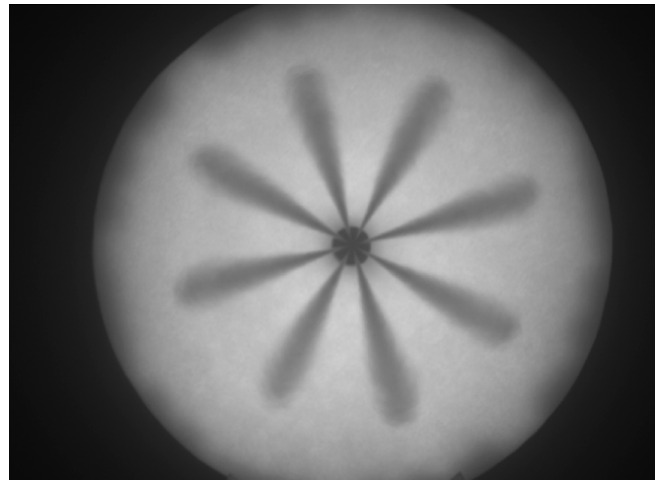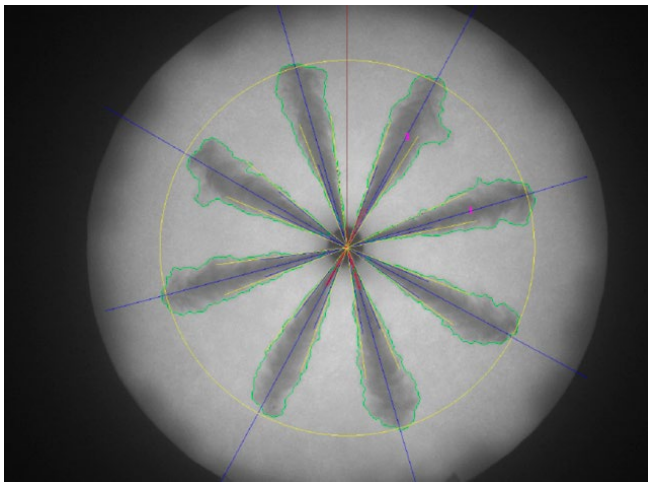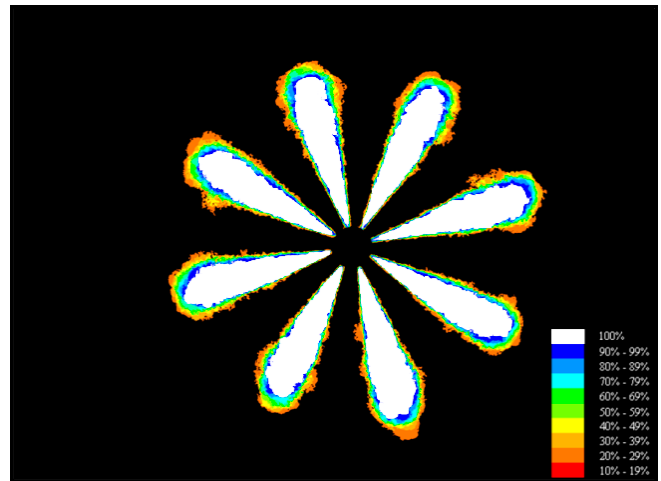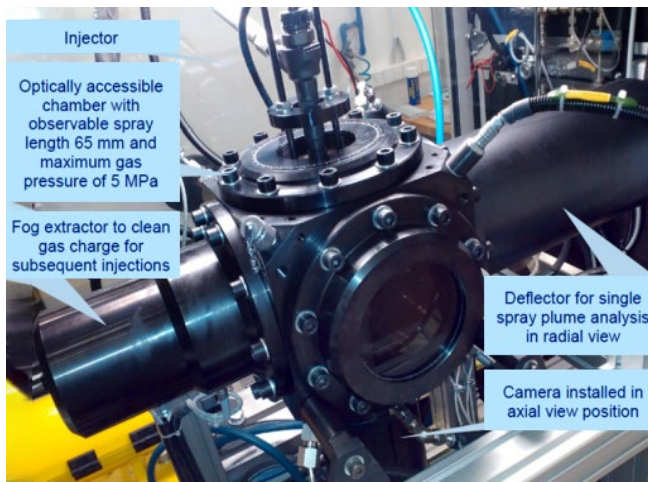
FIGURE 3: Cold pressure vessel with optical access for high-pressure injector testing – top left subfigure presents layout of the experimental test rig while the other subfigures correspond to typical output from analysis of experimental data (e.g., liquid phase mass fraction, instantaneous and average liquid jet shape).

OBRÁZEK 3: Studená tlaková komora s optickým přístupem pro testování vysokotlakých vstřikovačů – horní levý obrázek ukazuje uspořádání zkušebního zařízení, zatímco ostatní obrázky odpovídají typickým výstupům z analýzy experimentálních dat (např. hmotnostní podíl kapalné fáze, okamžitý a průměrný tvar kapalného paprsku).

Additional parameter to be tested was the mesh refinement. As mentioned below, fine mesh resolution near injector nozzles was needed to predict correctly liquid spray penetration when using LES approach. However, such meshes are too large for full ICE cycle calculations. Hence, different meshes were compared.

4. MODEL CALIBRATION

Spray calibration was performed while using experimental data from injection test bench (c.f. top left subfigure in Figure 3). The injection test bench EFS ITB 240 R-CV is based on cold pressure vessel with optical access which allows for measurement of rate-of-injection profile, injected amount (mass), spray penetration, spray cone angle for liquid phase and variation of a spray plume for each nozzle. As it is a cold

vessel, only liquid phase properties can be evaluated. More information regarding this test equipment can be found in [27]. Example of selected results from injection test bench is presented in Figure 3, average spray penetration data of the target injector are shown in Figure 4 (red curves). The tested injector is the BOSCH 0445110 369 B004 which is applied in AVL SCRE engine (c.f. Table 1 and Figure 1).

The cold pressure vessel was modeled in CFD code [36] to fine-tune the spray sub-model. As LES approach is adopted, complete geometry model was created – results from all injector holes were averaged and these data were compared with averaged data from experiments. Injection event was calculated in CFD code (initial and boundary conditions were transferred from experimental data) and selected spray model constants were varied to obtain the best match between simulation
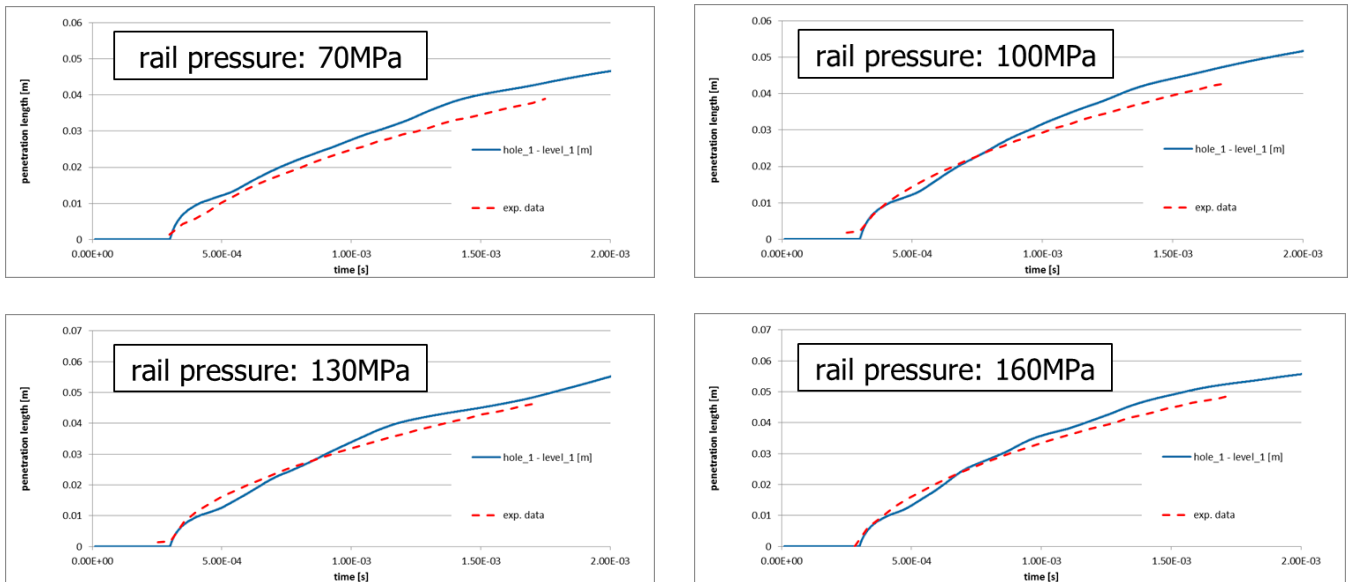
Application of Predictive Combustion Model to CI ICE based on LES and Chemical Kinetics
OLDŘICH VÍTEK, VÍT DOLEČEK, MARCEL DIVIŠ, JAN MACEK

MECCA 02 2018 PAGE 23

FIGURE 4: Comparison between measured data and calibrated LES spray model at different injection pressure levels while using data from cold pressure vessel – penetration length of liquid phase is plotted as function of time; LES spray model calibration was performed at injection pressure of 160 MPa.

OBRÁZEK 4: Srovnání mezi naměřenými daty a kalibrovaným LES modelem paprsku při různých úrovních vstřikovacího tlaku s využitím dat ze studené tlakové komory – penetrační délka pro kapalnou fázi je vynesena jako funkce času; LES model paprsku byl zkalibrován pro vstřikovací tlak 160 MPa.

and measured data (c.f. Figure 4). The calibration procedure was performed at pressure level of 160 MPa only, hence the data presented in Figure 4 for other pressure levels (70, 100 and 130 MPa) correspond to predictive ability of LES spray model. The match between simulation and measurement was considered satisfactory, hence the LES spray sub-model setting was transferred to full ICE model of the target engine.

Comparison of instantaneous spray pattern development in time domain between LES model prediction and experimental data is presented in Figure 5. As the shown data are instantaneous and as the length-scale of the figures is not the same (simulation vs. experiments), the figure is supposed to allow for qualitative comparison only – both the spray shape (including irregularities of each spray plume) and spray cone angle seem to be similar, hence confirming good performance of the LES spray model.

After a lot of testing and fine-tuning, the main conclusion from LES spray calibration is that the most critical factor is the mesh – it has to capture very small flow structures developing close to primary break-up zone (this concerns both length scale and time scale). Hence a lot of refinement was needed along each spray nozzle axis. Once the suitable mesh was created, the LES spray model calibration was relatively straightforward when C_2 constant of the WAVE model [28, 29] was the main parameter to influence the model performance and its final value was set to be 55 (and it was kept constant for all LES calculations).

As the combustion model is based on chemical kinetics, there are no parameters to be tuned with respect to combustion modelling. Selected chemical mechanism is based on a reduced n-heptane scheme containing 34 species and 64 reactions (the mechanism is in-house AVL one, which combines older reduced n-heptane scheme with Zeldovich extended NO mechanism). After spray model calibration was finished, the only other tuning parameter was a global heat transfer multiplier. It was necessary to adjust that due to the fact that LES heat wall transfer in CFD environment is a bit problematic. Hence, global heat transfer scaling approach was adopted to match total rejected heat, which was estimated by 0-D/1-D model.

5. DISCUSSION OF RESULTS

The most important results in terms of LES 3-D CFD combined with chemical kinetics for the case of CI ICE are presented in this section. The predicted data are compared with experimental/reference ones – the reference data correspond to calibrated 0-D/1-D model created in SW tool [37]. The reference data can give reasonable values of many integral data, however the prediction of pollutant formation (e.g., NO_x – c.f. Figure 14) represents only a rough estimate. Based on that, most of the figures consist of graphs representing global/integral parameters.
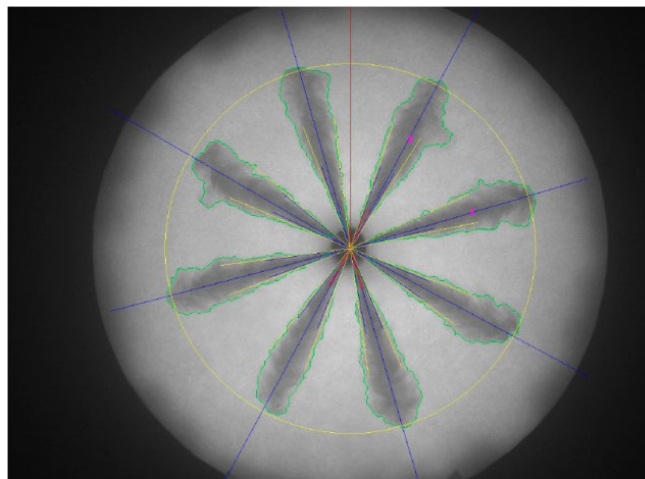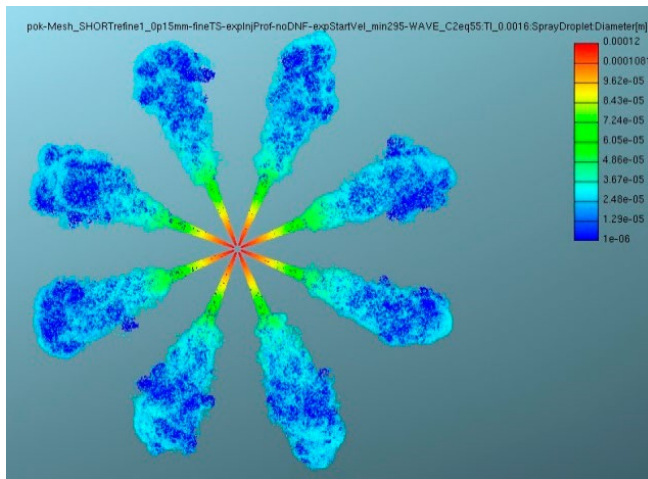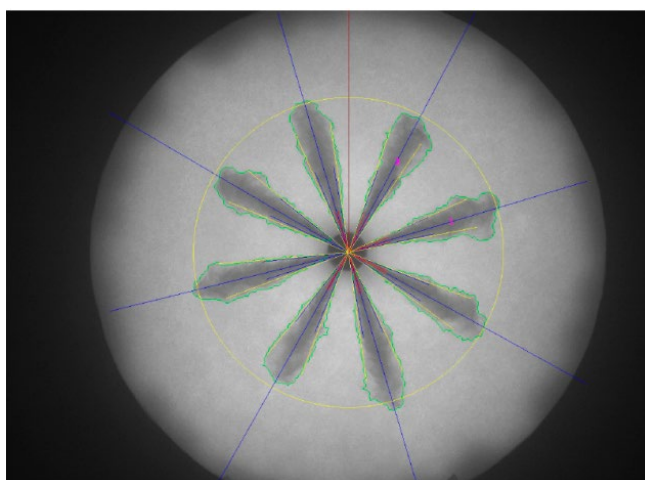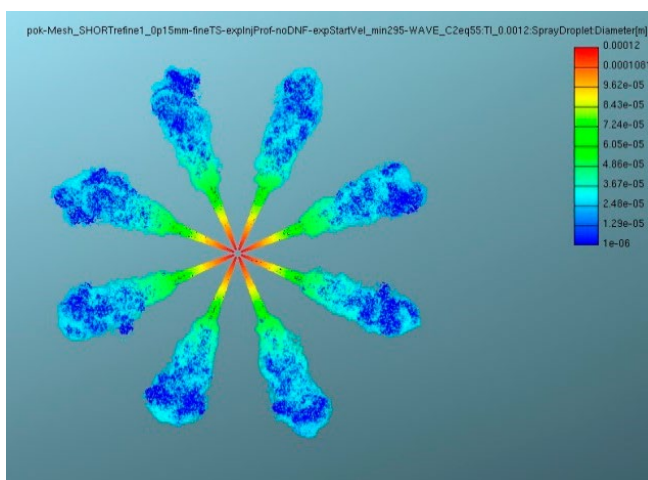
Application of Predictive Combustion Model to CI ICE based on LES and Chemical Kinetics
OLDŘICH VÍTEK, VÍT DOLEČEK, MARCEL DIVIŠ, JAN MACEK
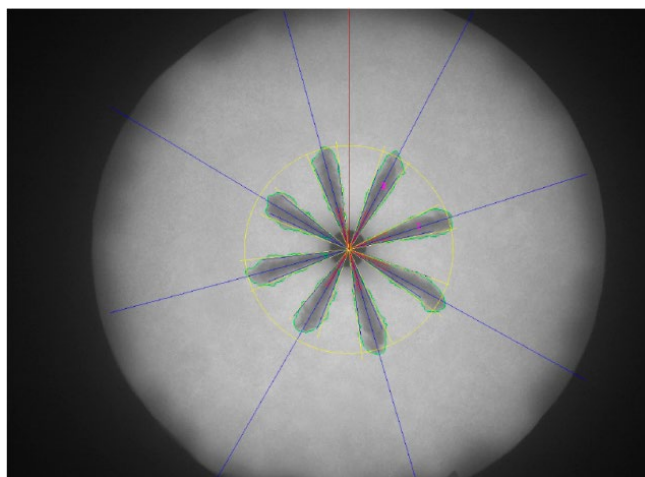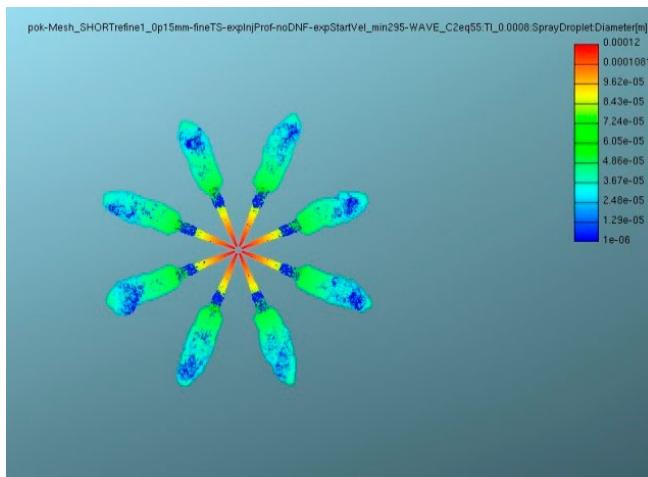
MECCA 02 2018 PAGE 24

FIGURE 5: Calibrated LES spray model performance – spray pattern development in time domain at injection pressure of 160 MPa (time instances of 0.4, 0.8 and 1.2 ms), left column corresponds to LES simulation while right column represents experimental data of a selected instantaneous injection shot (the figures are not scaled to match the length scale, hence only qualitative comparison is possible – penetration length comparison is shown in in Figure 4, bottom right subfigure).

OBRÁZEK 5: Chování kalibrovaného LES modelu paprsku – vývoj tvaru paprsku v časové doméně pro vstřikovací tlak 160 MPa (časy 0.4, 0.8 a 1.2 ms), levý sloupec odpovídá simulaci LES, zatímco pravý sloupec reprezentuje experimentální data odpovídající zvolenému okamžitému výstřiku (obrázky si neodpovídají z hlediska délkového měřítka, a tedy je možné jenom kvalitativní srovnání – porovnání doletu paprsku je ukázáno na Obrázku 4, pravý dolní diagram).
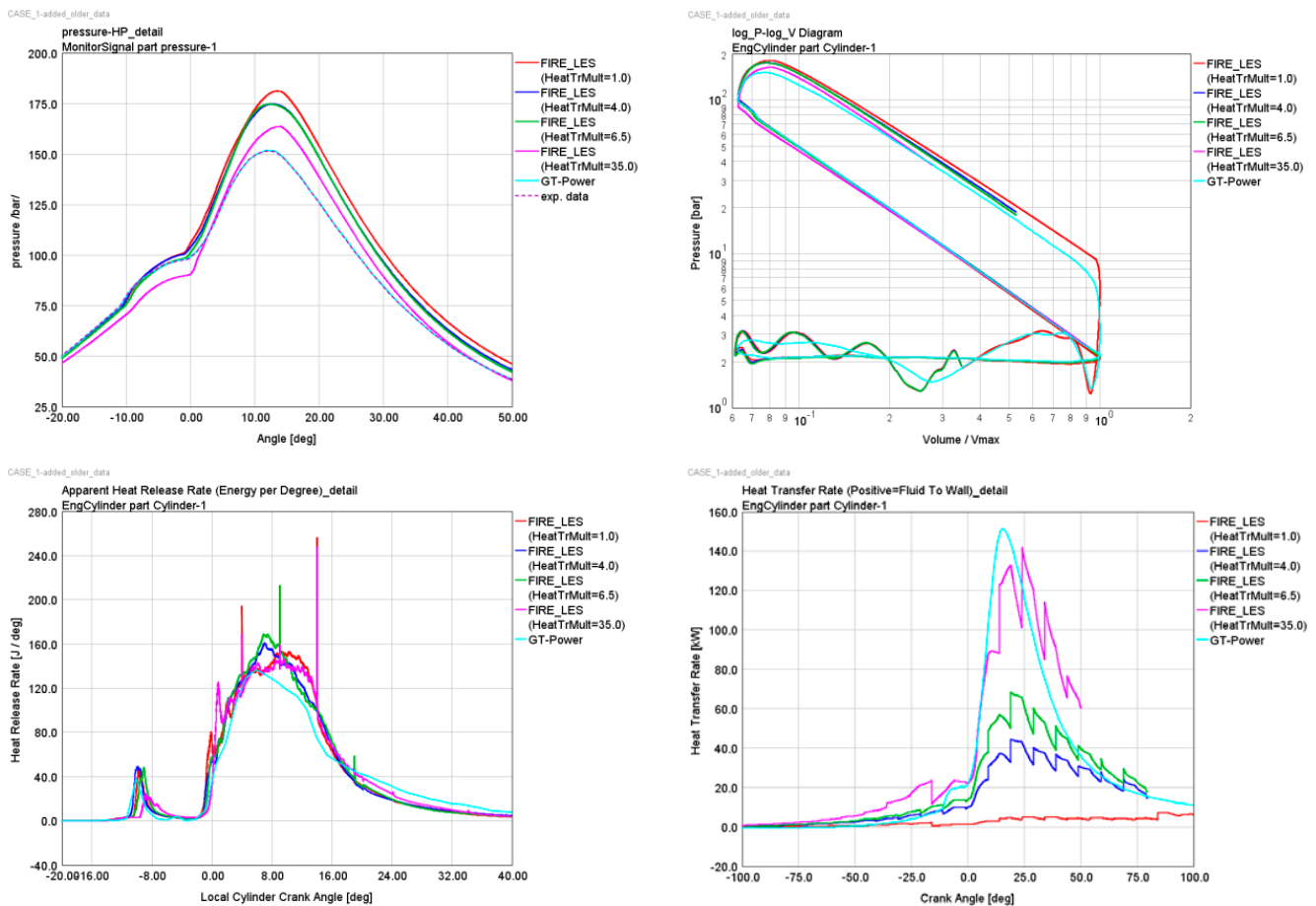
FIGURE 6: Influence of global heat transfer multiplier: comparison between measured/reference data (dashed magenta curve – experimental data, light blue curve – calibrated 0-D/1-D model) and LES CFD simulation for the operating point 'Case 1' (c.f. Table 3) – the following parameters are plotted as a function of engine crank angle: in-cylinder pressure, logarithmic diagram of pressure and volume, rate of heat release, in-cylinder heat transfer (to walls).

OBRÁZEK 6: Vliv globálního násobitele pro přestup tepla: srovnání mezi naměřenými/referenčními daty (čárkovaná fialová křivka – experimentální data, světle modrá křivka – kalibrovaný 0-D/1-D model) a LES CFD simulací pro pracovní bod „Case 1" (viz Tabulka 3) – následující parametry jsou zobrazeny jako funkce úhlu pootočení klikového hřídele: tlak ve válci, logaritmický diagram tlaku a objemu, rychlost vývinu tepla, přestup tepla (do stěn) ve válci.

During the model calibration phase, many calculations with different global heat transfer multipliers were calculated. Hence, it was decided to present its influence – this is shown in Figure 6. As expected, the global heat transfer scaling has significant impact on in-cylinder pressure. On the other hand, its influence on ROHR is relatively minor – higher values lead to slightly longer ignition delay, however ROHR shape is almost unaffected. This can be explained by the fact that the combustion process takes place in locations which are relatively distanced from combustion chamber walls. Hence, increased wall heat transfer has almost no effect on local temperature which controls chemical kinetics. Based on that, global heat transfer scaling is suitable for adjusting total energy balance in a combustion chamber and to match compression pressure curve. Final comment concerns the shape of instantaneous global heat transfer rate (Figure 6,

bottom right subfigure) – its qualitative trend corresponds reasonably well with Woschni formula applied in 0-D/1-D model. However, quantitative values are different (this was to be expected) and there are 'big jumps' – these correspond to re-zone procedures (i.e., switching between different mesh data sets). It seems that 3-CFD LES calculations have tendency to underestimate total heat transfer rate during combustion phase (i.e., when there is high temperature inside a combustion chamber). After analyzing all data from sensitivity studies, global heat transfer multiplier was set to be 4.0 and kept constant (during the whole cycle calculation and also for all tested cases from Table 3).

It is well known that LES simulations need proper mesh resolution to capture large turbulent eddies. When modelling interaction between liquid phase (fuel jet) and gaseous phase (in-cylinder charge), the LES approach needs to resolve
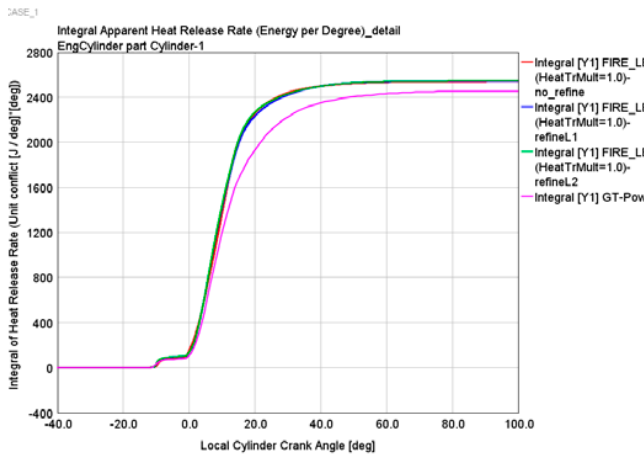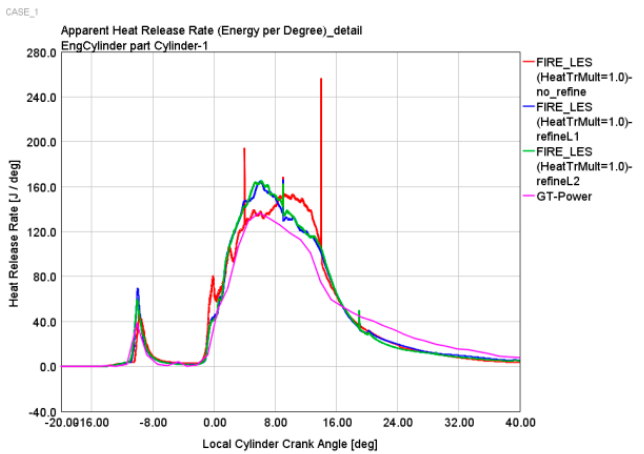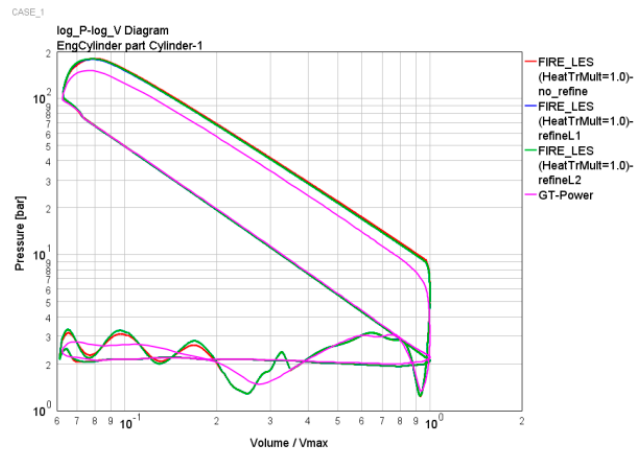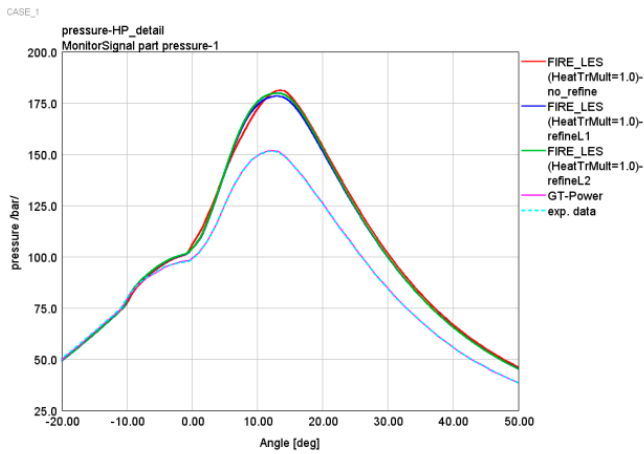
FIGURE 7: Influence of mesh refinement: comparison between measured/reference data (dashed light blue curve – experimental data, magenta curve – calibrated 0-D/1-D model) and LES CFD simulation for the operating point 'Case 1' (c.f. Table 3) – the following parameters are plotted as a function of engine crank angle: in-cylinder pressure, logarithmic diagram of pressure and volume, rate of heat release, heat release.

OBRÁZEK 7: Vliv zjemnění sítě: srovnání mezi naměřenými/referenčními daty (čárkovaná světle modrá křivka – experimentální data, fialová křivka – kalibrovaný 0-D/1-D model) a LES CFD simulací pro pracovní bod „Case 1" (viz Tabulka 3) – následující parametry jsou zobrazeny jako funkce úhlu pootočení klikového hřídele: tlak ve válci, logaritmický diagram tlaku a objemu, rychlost vývinu tepla, vývin tepla.

small scales near primary break-up zone to model turbulent dispersion effects correctly. This was verified when tuning LES spray model (for the case of cold pressure vessel) as a lot of mesh refinement was needed along each injector nozzle center line. However, such mesh is too big when applied for the target engine. Moreover, in-cylinder charge is relatively hot, hence a strong evaporation effect leads to the fact that liquid fuel phase penetration is much shorter when compared with experiments in a clod pressure vessel. Based on that, it is a reasonable assumption that less mesh refinement can be applied for engine LES simulations.

Based on all above mentioned facts, it was decided to perform sensitivity study regarding the mesh refinement to obtain the best compromise between computational time and result quality. All the presented meshes have the same basic setting – c.f. Table 2. The difference among the meshes

is in refinement level along each nozzle center line. If there was to be the same mesh as the one applied during LES spray model calibration, 'level 3' mesh would be required (the label 'refineL3'). However, such a mesh would be too big (more than 100M cells) and AVL FIRE cannot handle that for the case of a movable mesh for ICE calculations. Hence, lower refinement levels were tested – 'level 2' (label 'refineL2'; cca 41.6M cells at TDC) and 'level 1' (label 'refineL1'; cca 14.6M cells at TDC). Later on, 2 additional meshes were added (label 'refineL0a' and 'refineL0b') – these have 'coarse' refinement similar to 'level 1' and they have cca 5M cells at TDC. The difference between those 2 meshes is in topology of refinement. It should be stressed that mesh refinement was applied only during injection and combustion phase of a 4-stroke ICE cycle.
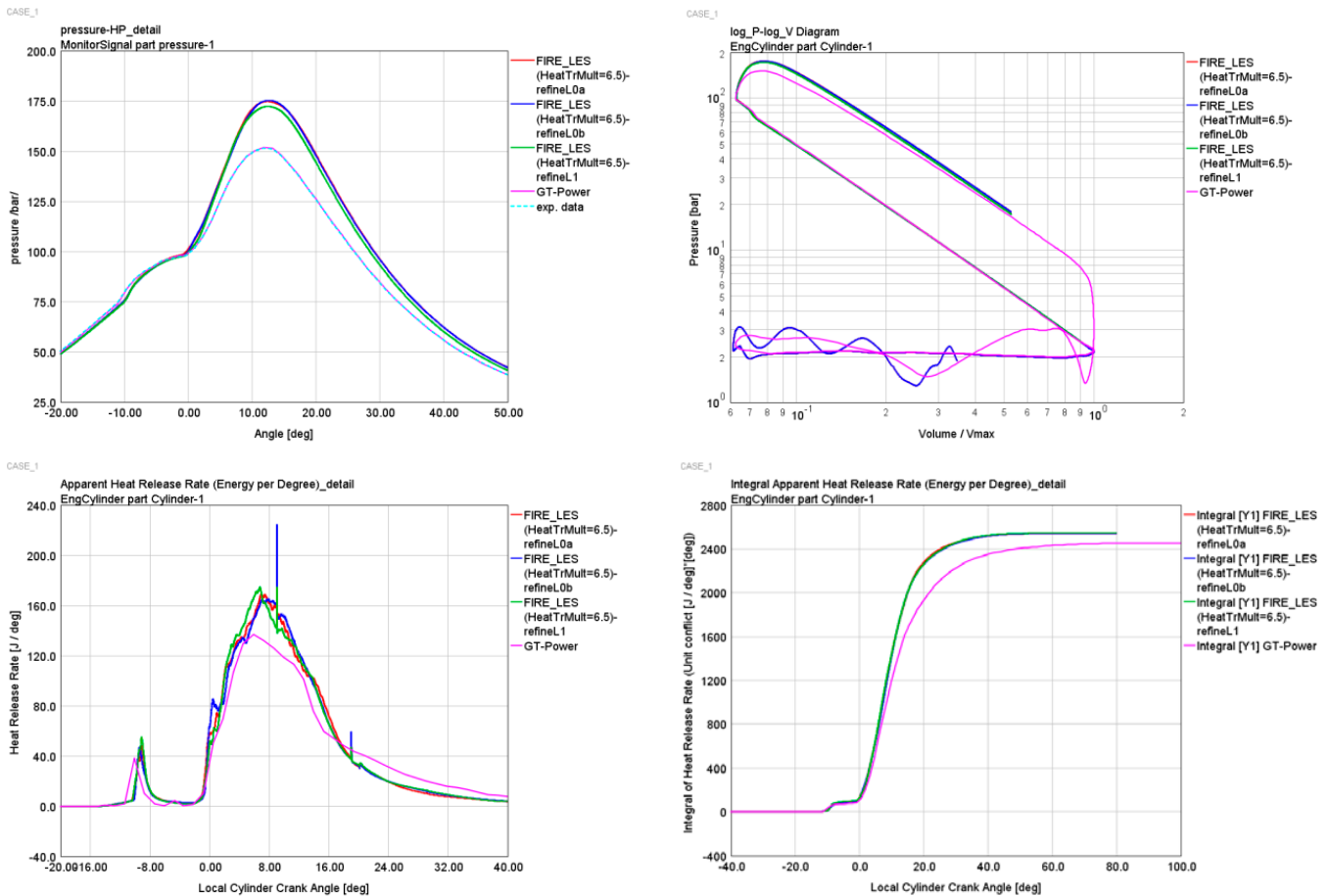
FIGURE 8: Influence of mesh refinement – additional fine-tuning: comparison between measured/reference data (dashed light blue curve – experimental data, magenta curve – calibrated 0-D/1-D model) and LES CFD simulation for the operating point 'Case 1' (c.f. Table 3) – the following parameters are plotted as a function of engine crank angle: in-cylinder pressure, logarithmic diagram of pressure and volume, rate of heat release, heat release.

OBRÁZEK 8: Vliv zjemnění sítě – další jemné doladění: srovnání mezi naměřenými/referenčními daty (čárkovaná světle modrá křivka – experimentální data, fialová křivka – kalibrovaný 0-D/1-D model) a LES CFD simulací pro pracovní bod „Case 1" (viz Tabulka 3) – následující parametry jsou zobrazeny jako funkce úhlu pootočení klikového hřídele: tlak ve válci, logaritmický diagram tlaku a objemu, rychlost vývinu tepla, vývin tepla.

Comparison of basic mesh (label 'no_refine', cca 2.5M cells at TDC) with refinement of 'level 1' and 'level 2' is presented in Figure 7. Although pressure traces are similar, there is a visible difference in rate of heat release – both refined meshes are closer to reference data when compared with basic mesh. This mainly concerns the main combustion phase when rate of heat release approaches its maximal value. It is interesting to note that ignition delay is almost independent of mesh refinement. Moreover, heat release peak due to pilot injection is very similar for all presented cases.

Due to the number of cells, calculations with meshes of 'level 1' and 'level 2' were massively slower when compared to basic mesh case. Moreover, additional problems were experienced with 'level 2' mesh due to memory limitations. Hence, additional 2 meshes were created ('refineL0a' and 'refineL0b') to search for the optimal solution in terms of computational time and result quality. Comparison of these 2 new meshes with 'level 1' mesh is shown in Figure 8. Both new meshes lead to results very similar to 'level 1' refinement, however they are much faster due to significantly lower number of cells. As the mesh 'refineL0a' seems to be slightly better than 'refineL0ab', it was selected as the final mesh which was applied for all subsequent CFD calculations. If there is no mesh label in figures or if the mesh label is 'final_version', the mesh 'refineL0a' was applied.

Although this paper is solely focused on LES 3-CFD modeling in combination with chemical kinetics, RANS approach was also tested. The RANS spray model was calibrated in the same way as the LES one (described above in section 'Model Calibration') while using the basic LES mesh –
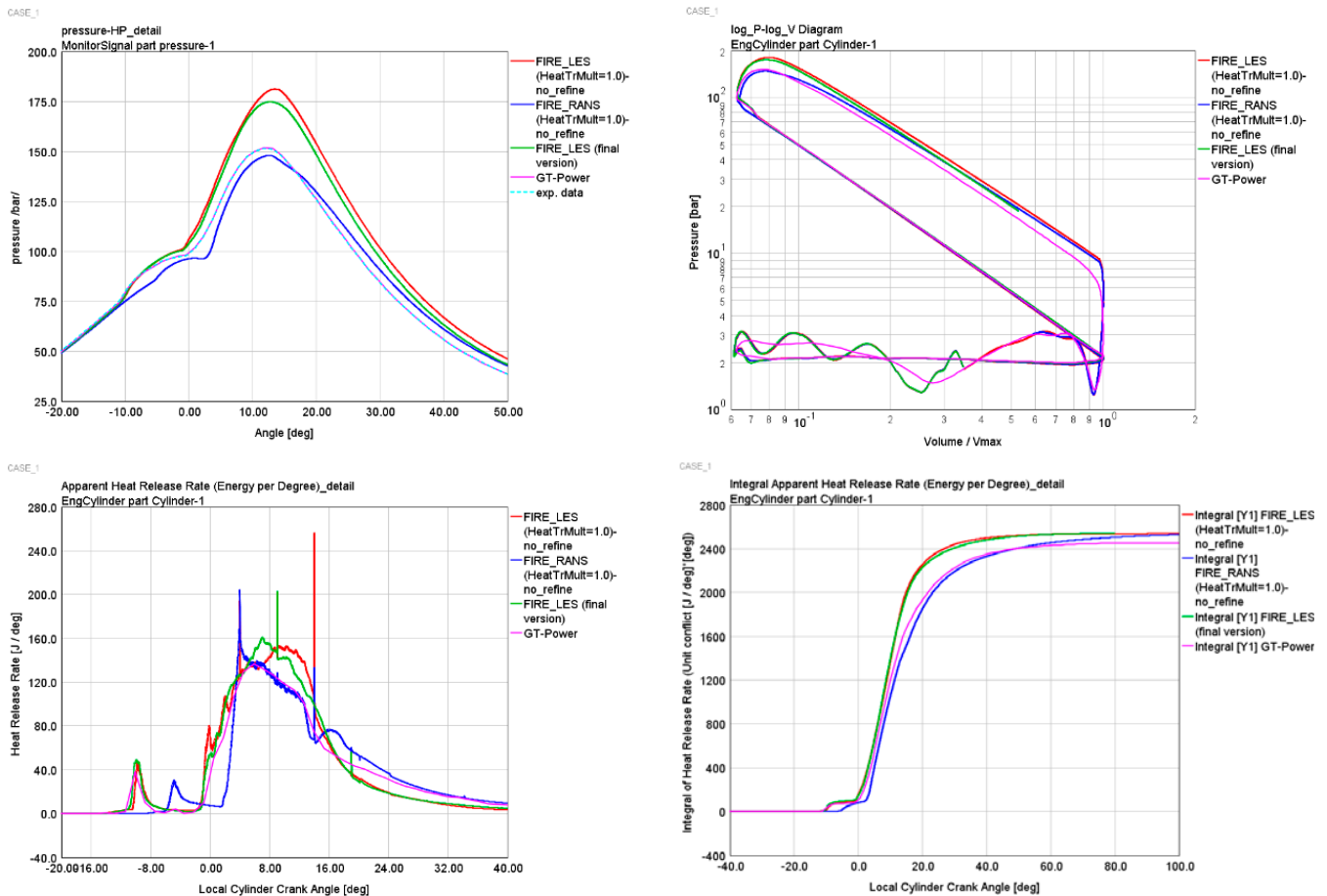
Application of Predictive Combustion Model to CI ICE based on LES and Chemical Kinetics
OLDŘICH VÍTEK, VÍT DOLEČEK, MARCEL DIVIŠ, JAN MACEK

MECCA 02 2018 PAGE 28

FIGURE 9: Comparison of LES vs. RANS between measured/reference data (dashed light blue curve – experimental data, magenta curve – calibrated 0-D/1-D model) and LES CFD simulation for the operating point 'Case 1' (c.f. Table 3) – the following parameters are plotted as a function of engine crank angle: in-cylinder pressure, logarithmic diagram of pressure and volume, rate of heat release, heat release.

OBRÁZEK 9: Srovnání LES vs. RANS mezi naměřenými/referenčními daty (čárkovaná světle modrá křivka – experimentální data, fialová křivka – kalibrovaný 0-D/1-D model) a LES CFD simulací pro pracovní bod „Case 1" (viz Tabulka 3) – následující parametry jsou zobrazeny jako funkce úhlu pootočení klikového hřídele: tlak ve válci, logaritmický diagram tlaku a objemu, rychlost vývinu tepla, vývin tepla.

it has to be stressed that no RANS meshes were created, hence the applied meshes were possibly too fine for RANS calculations. Once the RANS spray model was calibrated, it was transferred to full cycle ICE model and the 'Case 1' (c.f. Table 3) was calculated using the basic LES mesh (label 'no_refine'). The only differences between LES setup and RANS one are the following: turbulence model (LES vs k-z-f RANS), wall treatment approach and spray model setting (different model constants, mainly C_2, and activated option 'turbulent dispersion model') – all other settings (including time step) were the same. The comparison between LES and RANS is plotted in Figure 9 – mainly the difference between red curve (LES) and dark blue one (RANS) is of importance. RANS model strongly overestimates ignition delay and the shape of the rate of heat release curve is significantly different

when compared with reference data. On the other hand, the late combustion phase (more than 80% of in-cylinder fuel was burnt) is captured a bit better when compared with LES approach. It should be emphasized that no special effort was put to improve RANS results, hence there might be a potential for additional improvement. However, the main conclusion is that LES provides better results – the authors believe that the main reason behind that statement is better turbulence modelling of LES approach which leads to higher quality prediction of important phenomena (mainly mixing/diffusion and interaction between liquid phase and gaseous one).

After initial testing (based on sensitivity studies) was finished, the model setup was finalized regarding mesh properties (mesh 'refineL0a') and global heat transfer multiplier (value 4.0) – this is described above and it can be considered as

Application of Predictive Combustion Model to CI ICE based on LES and Chemical Kinetics
OLDŘICH VÍTEK, VÍT DOLEČEK, MARCEL DIVIŠ, JAN MACEK
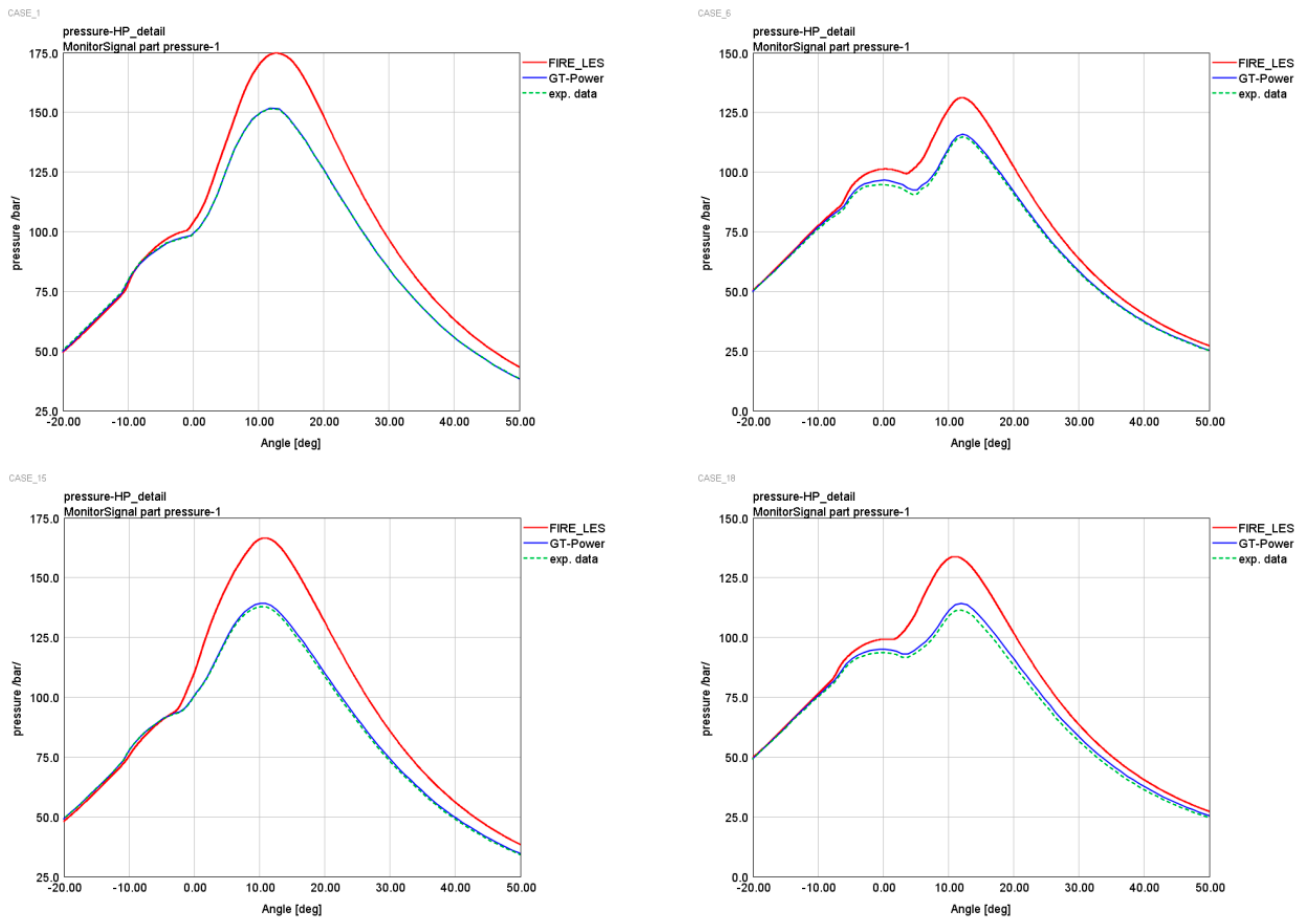
MECCA   02 2018   PAGE 29

FIGURE 10: Comparison between measured data (green curve) and LES CFD simulation (red curve) for all considered engine operating points (c.f. Table 3) when top left subfigure corresponds to 'Case 1' and bottom right subfigure represents 'Case 18' – in-cylinder average pressure of HP phase is plotted as a function of engine crank angle.

OBRÁZEK 10: Srovnání mezi naměřenými daty (zelená křivka) a LES CFD simulací (červená křivka) pro všechny uvažované pracovní body motoru (viz Tabulka 3), kdy levý horní obrázek odpovídá bodu „Case 1", zatímco pravý dolní obrázek reprezentuje bod „Case 18" – střední tlak ve válci pro vysokotlakou část je vynesen jako funkce úhlu pootočení klikového hřídele.

model fine-tuning. Then the model was applied to calculate all the cases from Table 3. As mentioned above, the 'Case 1' was used for model fine-tuning – hence, calculated data for all other cases represent predictive ability of the model. The results are shown in Figure 10, Figure 11 and Figure 14. Pressure traces are plotted in Figure 10 and the general trend is that the pressure is significantly over-predicted. However, ROHR curves (Figure 11) show relatively good match between prediction and reference data – when looking at details, predicted ROHR is slightly faster during early phase and during very late phase of main combustion process while energy release of pilot injection is captured reasonably well. Based on long-time experience with thermodynamic simulations, the following conclusion is made: the ROHR curves are too similar (when compared with reference data) to explain the

large over-shoot of predicted in-cylinder pressure. Hence, detailed analysis was performed to find the reason behind that. Important data for the 'Case 1' are shown in Figure 12 while very similar figures can be presented for all other cases – due to that, they are omitted as qualitative trends are the same for all cases.

Pressure data in Figure 12 confirm that gas exchange phase and compression stroke are predicted correctly and the difference arises during combustion phase. When comparing total released energy (middle left subfigure of Figure 12), approx. 4% more chemical energy is released for the case of the CFD simulation – this is related to the fact that that complex CI engine fuel is represented by n-heptane. Hence, if the same fuel mass is injected, there is more energy to be released. It was decided not to lower injected mass
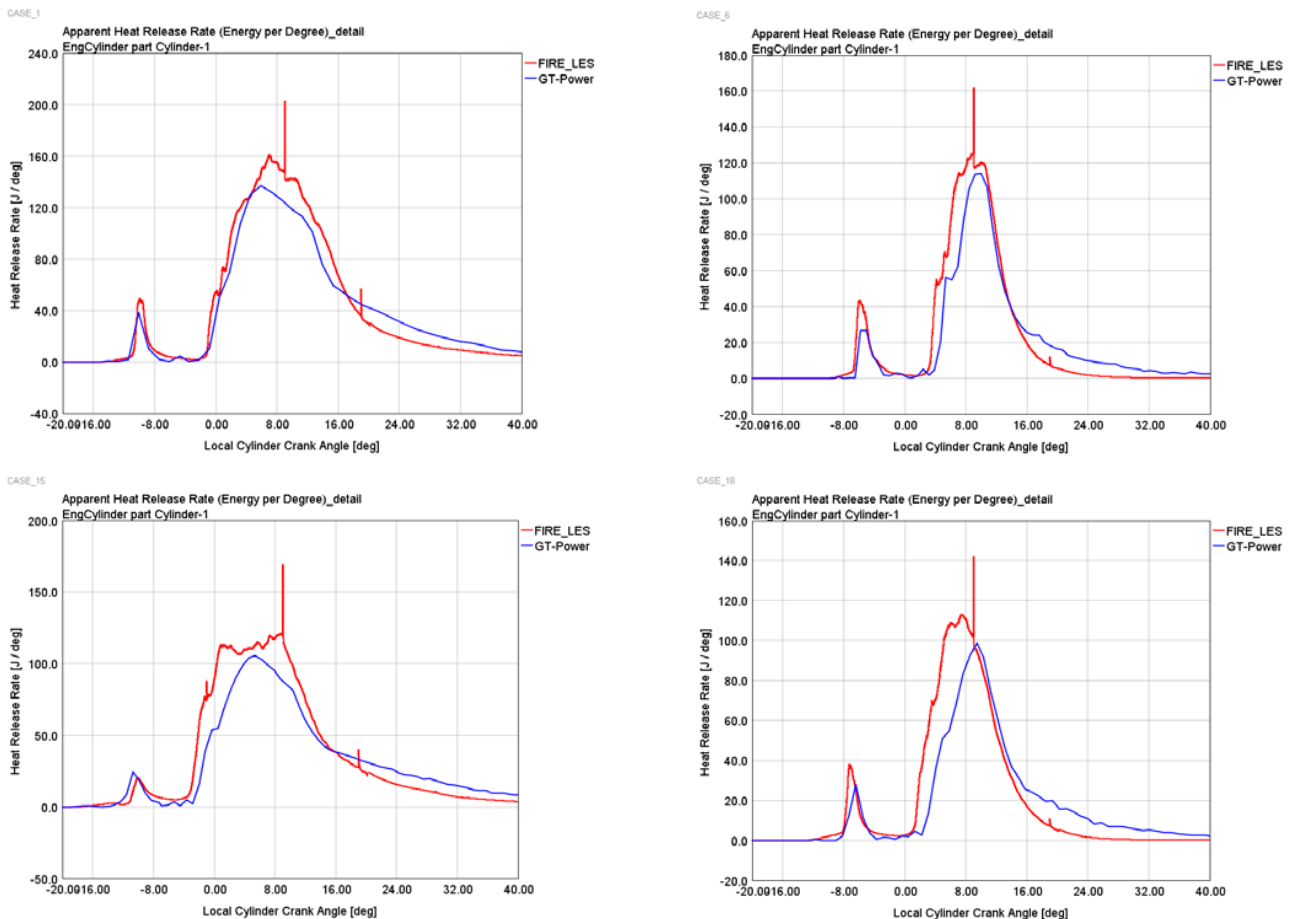
Application of Predictive Combustion Model to CI ICE based on LES and Chemical Kinetics
OLDŘICH VÍTEK, VÍT DOLEČEK, MARCEL DIVIŠ, JAN MACEK

MECCA 02 2018 PAGE 30

FIGURE 11: Comparison between reference data (blue curve – calibrated 0-D/1-D model) and LES CFD simulation (red curve) for all considered engine operating points (c.f. Table 3) when top left subfigure corresponds to 'Case 1' and bottom right subfigure represents 'Case 18' – rate of heat release is plotted as a function of engine crank angle.

OBRÁZEK 11: Srovnání mezi referenčními daty (modrá křivka – kalibrovaný 0-D/1-D model) a LES CFD simulací (červená křivka) pro všechny uvažované pracovní body motoru (viz Tabulka 3), kdy levý horní obrázek odpovídá bodu „Case 1", zatímco pravý dolní obrázek reprezentuje bod „Case 18" – rychlost vývinu tepla je vynesena jako funkce úhlu pootočení klikového hřídele.

(to compensate higher specific chemical energy of n-heptane fuel) as it might influence spray development significantly. Predicted combustion is slightly faster (especially for low BMEP cases during early main combustion phase) and there is lower cooling effect during combustion phases (c.f. bottom right subfigure of Figure 6). All these phenomena lead to higher pressure increase (when compared with reference data). Another important factor is related to chemical composition of combustion products, hence thermodynamic properties. As it is clear from mass fraction diagrams of Figure 12, a bit more oxygen is consumed while les CO_2 and more H_2O is created during the combustion phase – this is (again) a consequence of application of n-heptane instead of complex diesel fuel. However, it can be shown that there is relatively small difference when comparing specific isobaric

capacities of all considered variants (presented in Figure 13). There are more complex chemical mechanisms (e.g., [30, 31, 32, 33]) for modelling of diesel fuel combustion, however they consist of significantly more species and chemical reactions, hence requiring much more computational time. Their application is not feasible for direct solution of chemical kinetics (as applied in the case of presented results) – such cases require pre-calculated chemical tables to achieve reasonable calculation times. To estimate the influence of the above mentioned effects, calibrated 0-D/1-D model was modified to take into account different calculation settings – the outcome of these simulations is shown in Figure 13. As it is clear from this figure, the above mentioned effects are primarily responsible for pressure over-shoot. However, when dealing with high BMEP cases, there is still visible difference
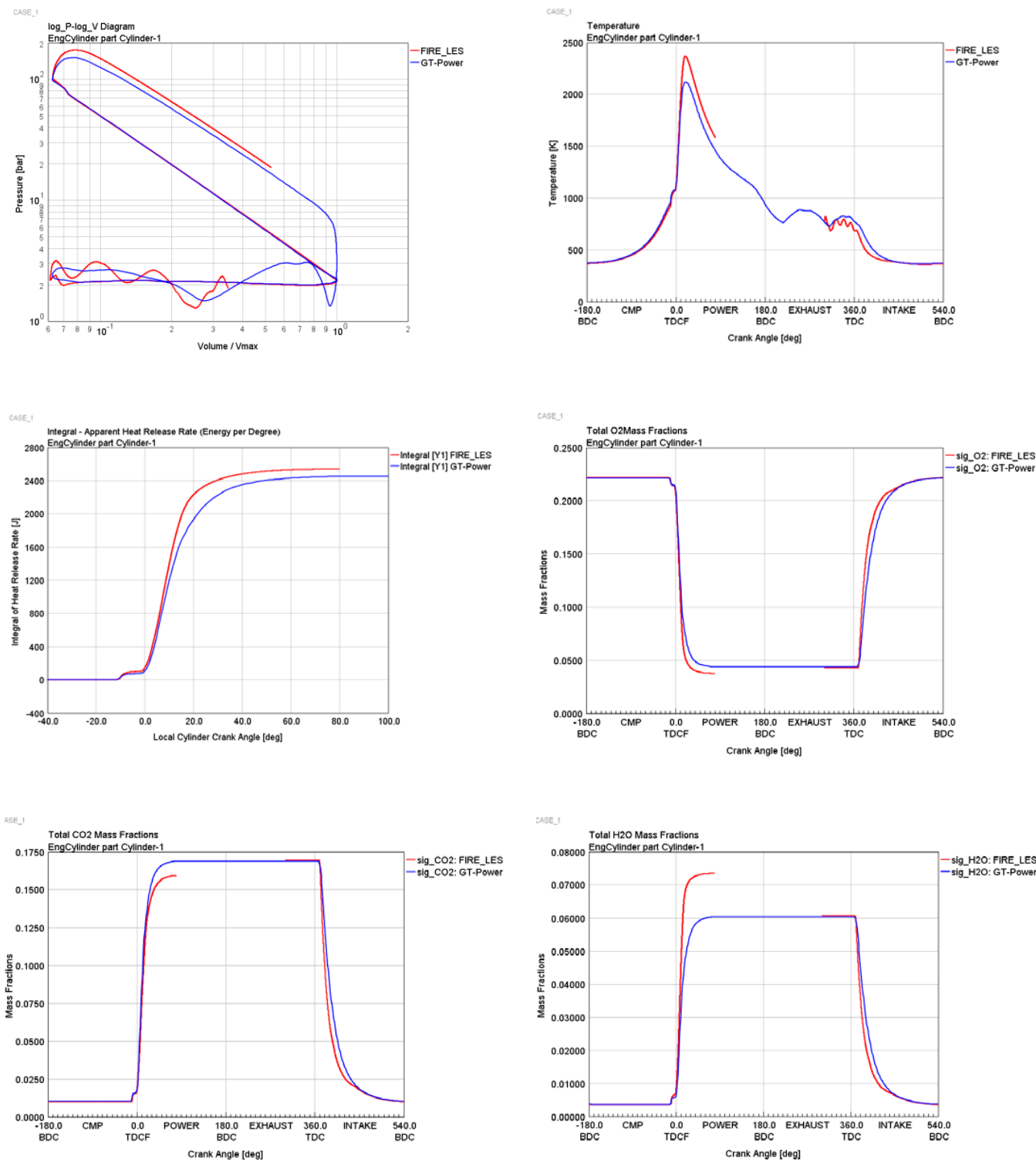
Application of Predictive Combustion Model to CI ICE based on LES and Chemical Kinetics
OLDŘICH VÍTEK, VÍT DOLEČEK, MARCEL DIVIŠ, JAN MACEK

MECCA 02 2018 PAGE 31

FIGURE 12: Comparison between reference data (blue curve – calibrated 0-D/1-D model) and LES CFD simulation (red curve) for the operating point 'Case 1' (c.f. Table 3) – the following parameters are plotted as a function of engine crank angle: logarithmic diagram of pressure and volume, in-cylinder average temperature, heat release, in-cylinder mass fraction of O_2, in-cylinder mass fraction of CO_2, in-cylinder mass fraction of H_2O.
OBRÁZEK 12: Srovnání mezi referenčními daty (modrá křivka – kalibrovaný 0-D/1-D model) a LES CFD simulací (červená křivka) pro pracovní bod „Case 1" (viz Tabulka 3) – následující parametry jsou zobrazeny jako funkce úhlu pootočení klikového hřídele: logaritmický diagram tlaku a objemu, průměrná teplota ve válci, vývin tepla, hmotností podíl O_2 ve válci, hmotností podíl CO_2 ve válci, hmotnostní podíl H_2O ve válci.
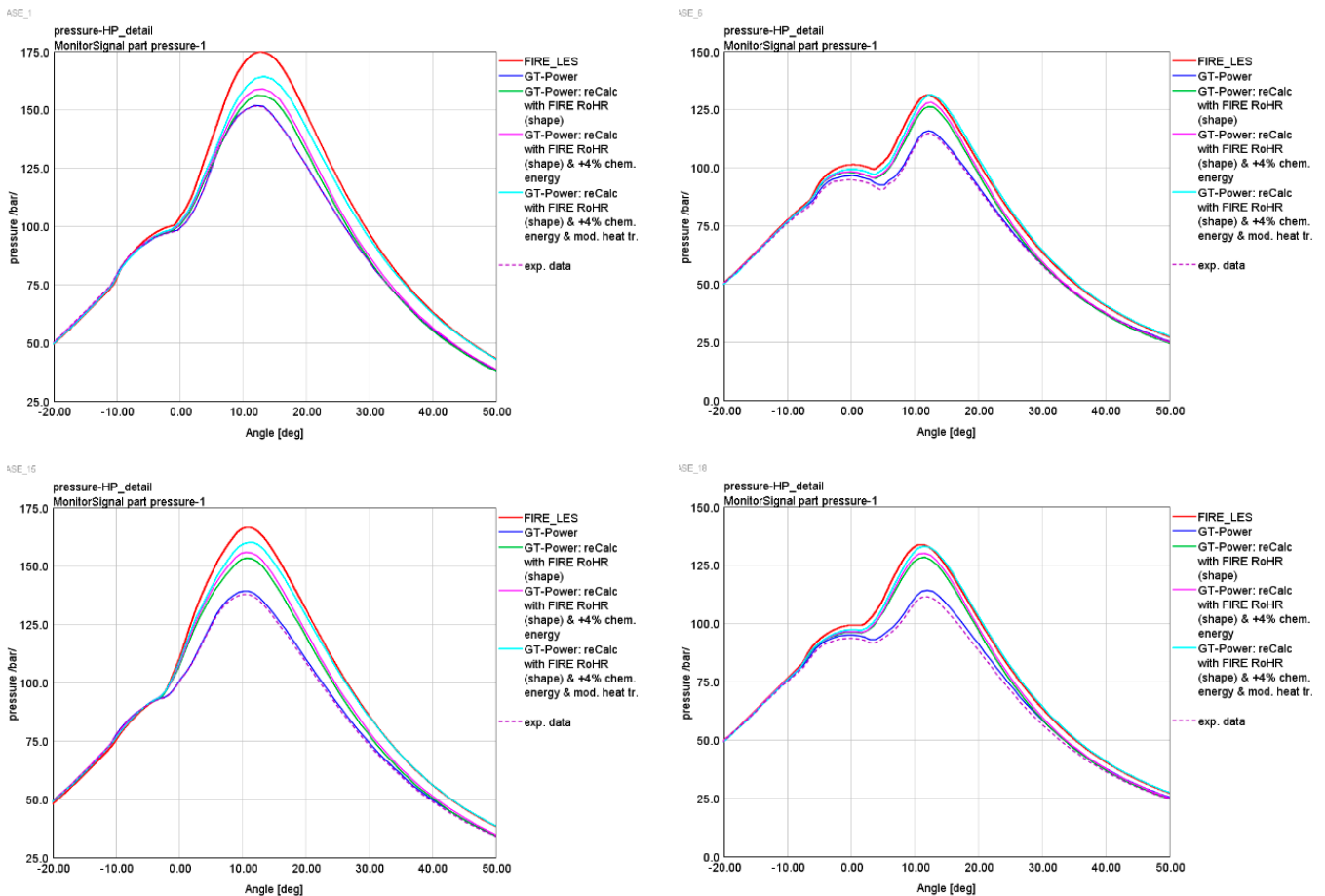
FIGURE 13: Influence of different calculation settings to explain pressure over-shoot of LES CFD calculation (red curve) when compared with reference data (dark blue curve) for all considered engine operating points (c.f. Table 3) when top left subfigure corresponds to 'Case 1' and bottom right subfigure represents 'Case 18' – in-cylinder average pressure of HP phase is plotted as a function of engine crank angle.
OBRÁZEK 13: Vliv různých nastavení simulace pro vysvětlení nadhodnocení tlaku ve válci pro LES CFD simulaci (červená křivka) při srovnání s referenčními daty (tmavě modrá křivka) pro všechny uvažované pracovní body motoru (viz Tabulka 3), kdy levý horní obrázek odpovídá bodu „Case 1", zatímco pravý dolní obrázek reprezentuje bod „Case 18" – střední tlak ve válci pro vysokotlakou část je vynesen jako funkce úhlu pootočení klikového hřídele.

between LES CFD and modified 0-D/1-D model (light blue curves in Figure 13), which takes into account different ROHR shape (transferred from LES CFD), +4% of released chemical energy and lower in-cylinder heat transfer. This difference is expected to be mainly related to different thermodynamic properties due to differences in chemical composition when comparing 3-D CFD approach (based on chemical kinetics) and 0-1/1-D one (based on chemical equilibrium).

When dealing with detailed combustion modeling of any ICE, pollutant formation is one the most important results of CFD simulations. In this particular case (diesel engine), NO_x and particulate matter (PM) are of primary interest. However, PM is difficult to predict as its physics and chemistry (related to its in-cylinder formation) is too complex. Hence, NO_x was tested versus experimental data. Instantaneous in-cylinder

NO_x (represented by its mass fraction) is shown in Figure 14. Obviously, experimental data (green curve) is represented by constant line as there is no direct in-cylinder measurement available. On the other hand, all simulation results are based on solving chemical kinetics of extended Zeldovich mechanism (c.f. [20, 22]). Although a lot of effort was put to calibrate predictive combustion model including NO_x formation for the case of 0-D/1-D model (dark blue curve – reference data), its NO_x prediction is relatively poor as 0-D in-cylinder approach cannot capture the physics of CI ICE combustion correctly. This leads to strong variations of instantaneous in-cylinder NO_x, which are not supported by LES 3-D CFD calculations (red curve). The CFD results are more consistent with measure data, which was to be expected, and they can follow the qualitative trends in the right way. However, the quantitative

values are over-predicted by factor between 2 and 3. Based on the above mentioned (regarding in-cylinder pressure/ temperature over-shoot), this is a logical consequence due to higher local temperature. NO$_x$ formation is strongly non-linear with respect to value of local temperature, which is a results of many complex phenomena. Hence, there is no guarantee that if 3-D CDF predicts correct in-cylinder pressure, calculated NO$_x$ would match experimental data
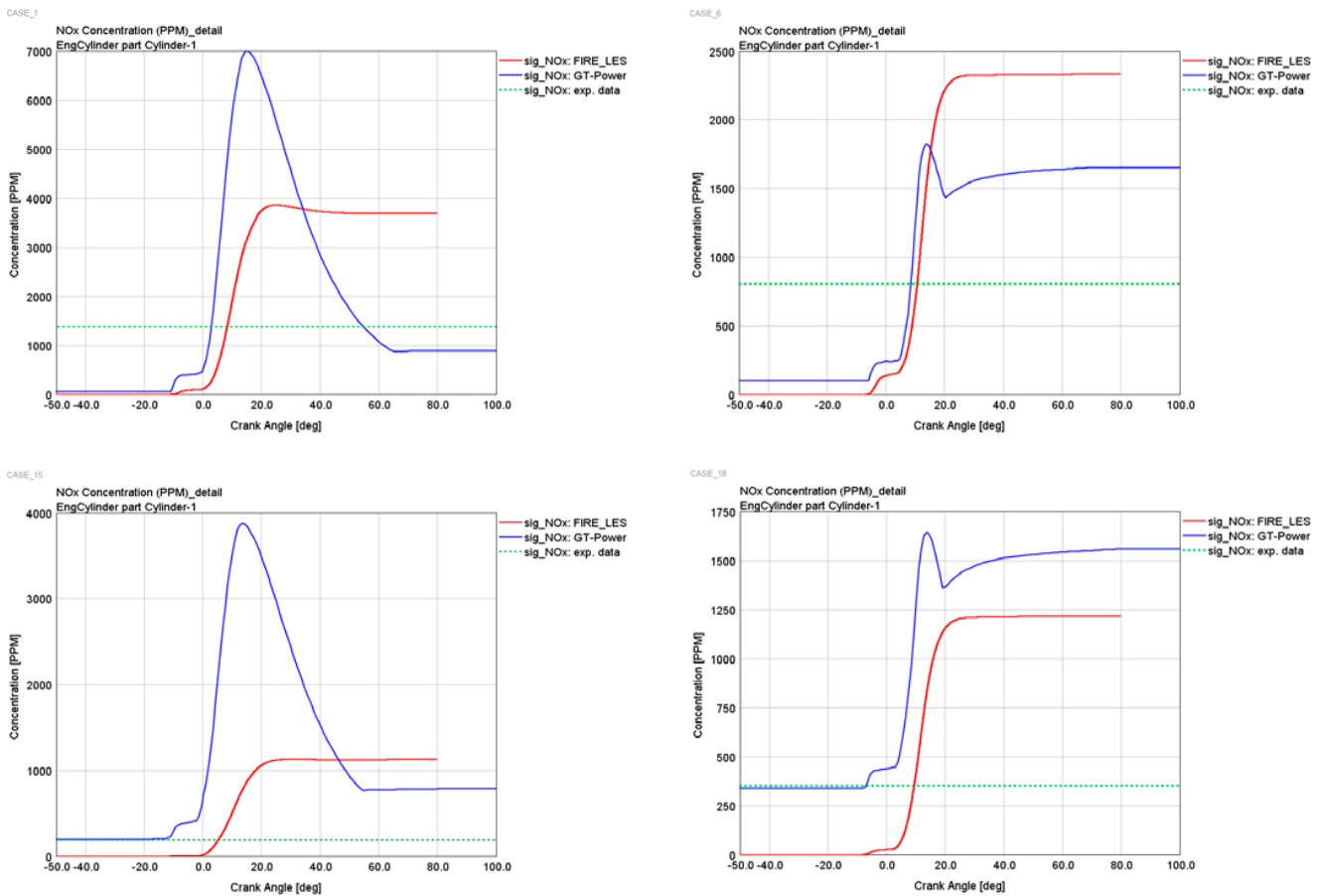

**FIGURE 14:** Comparison between measured/reference data (green curve – experimental data, blue curve – calibrated 0-D/1-D model) and LES CFD simulation (red curve) for all considered engine operating points (c.f. Table 3) when top left subfigure corresponds to 'Case 1' and bottom right subfigure represents 'Case 18' – in-cylinder NO$_x$ is plotted as a function of engine crank angle.

OBRÁZEK 14: Srovnání mezi naměřenými/referenčními daty (zelená křivka – experimentální data, modrá křivka – kalibrovaný 0-D/1-D model) a LES CFD simulací (červená křivka) pro všechny uvažované pracovní body motoru (viz Tabulka 3), kdy levý horní obrázek odpovídá bodu „Case 1", zatímco pravý dolní obrázek reprezentuje bod „Case 18" – NO$_x$ ve válci jsou vyneseny jako funkce úhlu pootočení klikového hřídele.

FIGURE 15: Comparison between operating point 'Case 1' (left column) and 'Case 6' (right column) in terms of detailed 3-D data representing the combustion phase – the following information is plotted in every subfigure: mass fraction of OH radical (top 2 cuts), iso-surface of constant OH radical (bottom left, color represents local temperature mapped onto iso-surface), liquid fuel space distribution (bottom right cut, color represents droplet size); different combustion phases are shown (due to different fuel injection timing of the considered operating points, corresponding subfigures do not have the same time/angle coordinate): pilot injection (1st row), phase between pilot injection and main injection (2nd row), early main injection (3rd row), middle of main injection (4th row).

OBRÁZEK 15: Srovnání mezi pracovními body „Case 1" (levý sloupec) a „Case 6" (pravý sloupec) z hlediska detailních 3-D dat reprezentujících fázi hoření – následující informace jsou vyobrazeny na každém obrázku: hmotnostní podíl OH radikálu (2 horní řezy), izoplocha konstantního OH radikálu (vlevo dole, barva odpovídá lokální teplotě, která je namapována na izoplochu), prostorové rozložení kapalné fáze (vpravo dole, barva odpovídá velikosti kapek); různé fáze spalování jsou ukázány (kvůli různému časování průběhu výstřiku paliva uvažovaných pracovních bodů nemají odpovídající si obrázky stejnou časovou/úhlovou souřadnici): pilotní vstřik (řádek 1), fáze mezi pilotním a hlavním výstřikem (řádek 2), úvodní fáze hlavního výstřiku (řádek 3), prostřední část hlavního výstřiku (řádek 4).
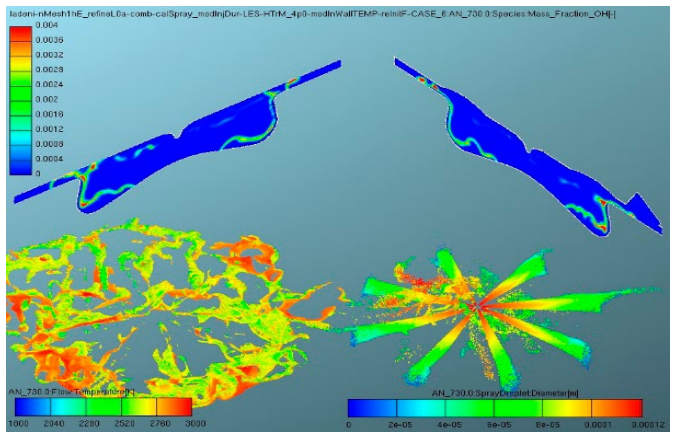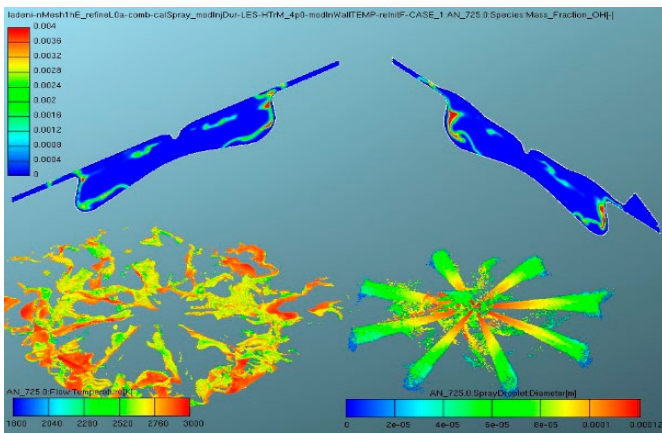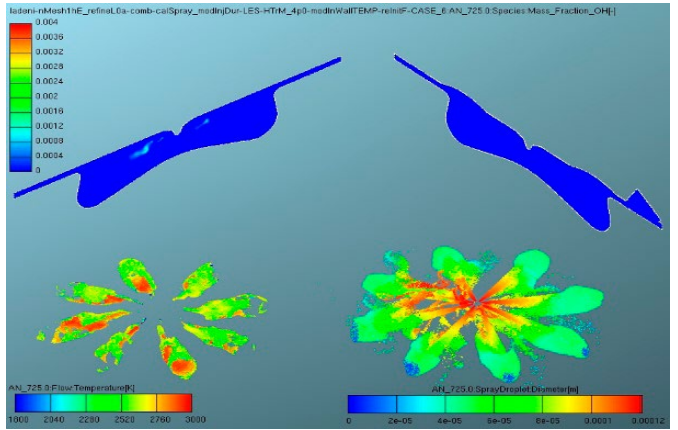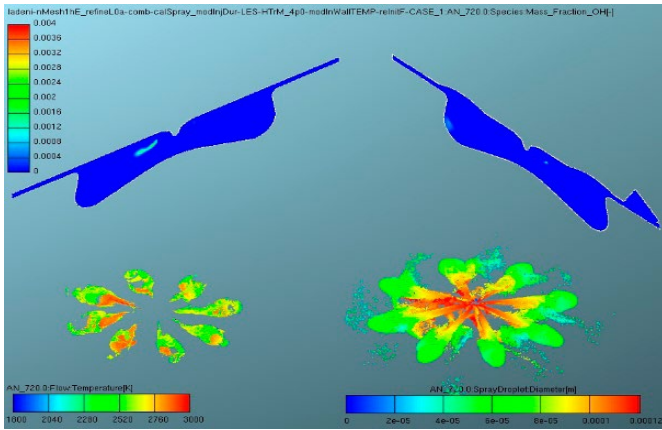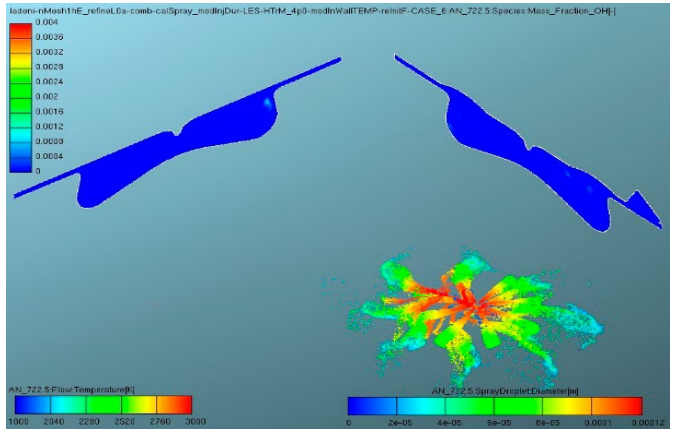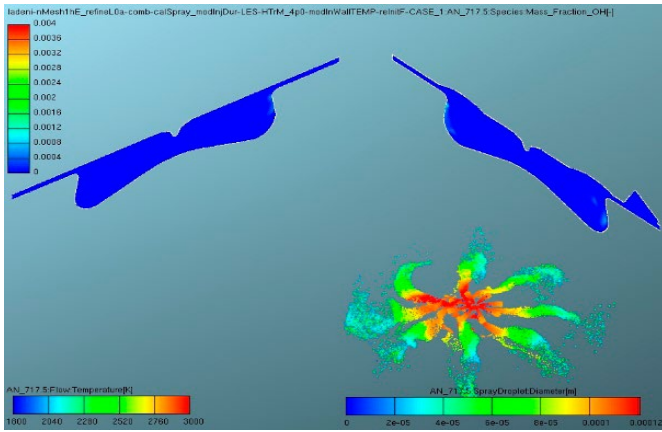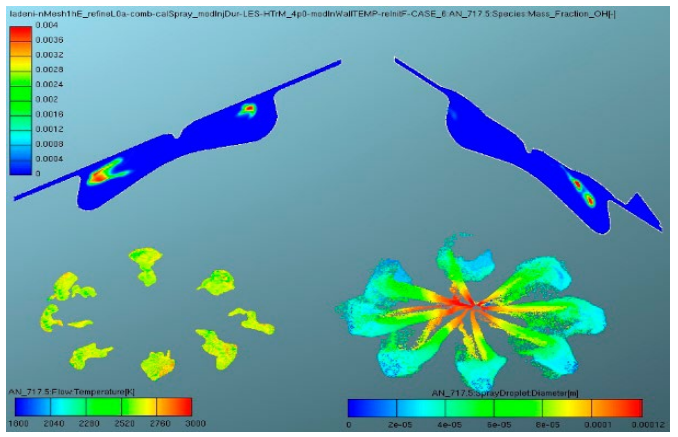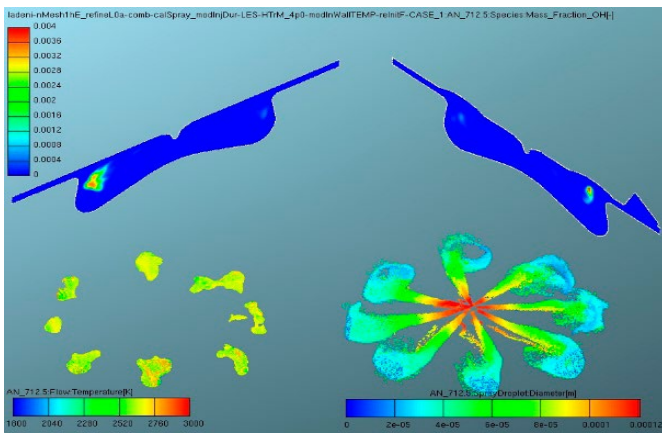
in a quantitative way. Concerning the shape of in-cylinder NOx fraction for LES CFD case, it suggests that NO_x is formed by relatively slow (kinetically controlled) chemistry without possibility to reach chemical equilibrium.

So far, integral data were analyzed as there are either experimental data or reference ones (calibrated 0-D/1-D model of the target engine) for comparison with 3-D CFD predictions. It is also interesting to look at space distribution of selected parameters to compare it with well-known knowledge of CI ICE combustion. This is done in Figure 15 for the case of combustion phase of 'Case 1'. The plotted data are intended to visualize locations with high chemical activity and to relate them to status of fuel jet. The former one is based on plotting OH radical while the latter one is represented by droplet space distribution including its size. Bottom left part of each subfigure of Figure 15 represents an iso-surface of constant OH radical concentration (selected by a user) to visualize a shape/topology of the flame while the color (mapped onto the iso-surface) corresponds to local temperature. It can be seen that peak temperature in burning zone is approx. 2700-2800 K, which is in a good correspondence with current knowledge of diesel combustion (c.f. [23]). The shape of burning zone follows spray shape during early phase of combustion process. Later on, the burning zone has a complicated shape while being clearly larger than the spray domain – this is a result of complex physics and chemistry taking place inside combustion chamber dominated by turbulent diffusion. Interaction of burning zone with large-scale swirling/squish motion and even with piston bowl is also important and it leads (in this particular case) to high chemical activity near outer walls of piston bowl.

Final comment concerns the CCV effects. It should be stressed that measured/reference data represent average cycle while LES CFD data corresponds to single-cycle realization. The experience from SI ICE simulations focused on CCV (c.f. [1, 2, 3]) is that the first calculated cycle can be far off from the average one. It should be stressed that the results presented in this paper correspond to single-cycle calculations only. On the other hand, CI ICEs are well-known to feature much less CCV (variation of max. in-cylinder pressure is below 2-5%) when compared with SI ICEs (variation of max. in-cylinder pressure can be even more than 20%). In this particular case, variation of max. in-cylinder pressure is below 2.5% while coefficient of IMEP variation is below 0.5%, hence there is little difference among all the instantaneous cycles – this applies for all considered cases from Table 3. There are not many literature sources dealing with CCV in CI ICEs (when compared with CCV in SI ICEs), however they support these statements – c.f. [34, 9].

The multi-cycle LES CFD calculations of the target engine are planned for the near future. However, different approach will be adopted as the direct solution of chemical kinetics (even if 'clustering' method is applied) is too slow. There is already a positive experience when detailed chemistry is represented by pre-calculated chemical tables – this makes the simulation approx. 4-times faster. This also allows for application of much more complex chemical mechanisms, hence dealing with some shortcomings of the approach described in this paper. On the other hand, there is still some work to be done as there are some technical problems related to that.

Based on available knowledge, diesel combustion CCV is primarily driven by variations of injector performance and ignition delay variability due to pressure/temperature variations. The former effect is usually low when modern high-pressure injectors are applied – c.f. [35], however this information was not available for the considered injector which may result in a necessity to re-run some experiments in cold pressure vessel. The latter phenomenon should be captured properly by LES 3-D CFD approach.

Based on the above mentioned, it is not expected that multi-cycle CFD calculations will lead to significantly different results when compared with the presented data. Hence, even if only single-cycle calculations were performed, the authors believe that they represent the average cycle reasonably well, thus presented conclusions are generally valid.

6. CONCLUSION

The paper deals with LES 3-D CFD modeling of CI ICE while main focus is put on combustion phase as chemical kinetics is applied to predict ROHR and NO_x formation. The LES once again proved to be a reliable tool when little fine-tuning of various sub-models is needed, hence confirming high predictive ability of LES approach in general. However, this comes with high computational cost as LES calculations are very time demanding. When chemical kinetics is applied while using relatively simple chemical mechanism based on n-heptane in combination with 'clustering' method to speed up the chemistry solution, it is even more time demanding.

Concerning the calibration procedure, fine-tuning of LES spray model in combination with proper 'LES-like' mesh is a critical step to correctly resolve interaction between liquid phase and gaseous one. It was found out that slightly coarser mesh can be applied for 'hot' CI ICE calculations when compared with 'cold' pressure vessel cases (related to LES spray calibration). The other important parameter to fine-tune is in-cylinder heat transfer due to the fact that correct boundary layer modeling in LES framework is problematic. However, this parameter has relatively low influence on ROHR prediction. Once these tuning parameters are fixed, no other modifications are needed.

Regarding the prediction of ROHR, the following can be stated. The ignition delay and the shape of ROHR is predicted relatively well. In some cases, simulated ROHR is slightly faster during the early part of main combustion phase while combustion of pilot injection is predicted correctly. Additionally, the very late phase of burning is (again) faster in CFD simulations when compared with measured/reference data. When comparing in-cylinder pressure traces, it can be seen that CFD data systematically 'over-shoot' measured ones during combustion phase. There are various reasons behind that. First, slightly faster simulated ROHR leads to higher in-cylinder pressure. Second, this effect is magnified by the fact that complex diesel fuel is modeled as n-heptane, which has a bit higher lower heating value (approx. +4%), hence more energy is released during combustion. Third, different fuel properties lead to different in-cylinder chemical composition, hence different thermodynamic properties. Fourth, even if global heat transfer was calibrated, instantaneous heat transfer during combustion phase is significantly lower when compared with Woschni formula prediction (which was applied in calibrated 0-D/1-D model of the target engine). Hence, suggesting that less energy is transferred to walls (of combustion chamber) when combustion takes place. All these factors contribute to pressure 'over-shoot'. These need to be addressed in future calculations to improve in-cylinder pressure prediction.

Dealing with NO_x formation, the qualitative trends match well experimental data. Instantaneous in-cylinder NO_x mass fraction follows expected trend of relatively slow chemistry, which becomes frozen during late phase of combustion process – this is in-line with well-known knowledge of CI ICE combustion. This trend cannot be properly captured by simple multi-zone models applied in 0-D/1-D SW tools. Concerning quantitative values, 3-D CFD overestimates NO_x values by factor between 2 and 3. The main reason seems to be related to higher local temperatures – this effect is mentioned/explained above (when explaining in-cylinder pressure 'over-shoot').

When looking at details of in-cylinder distribution of various thermodynamic parameters during combustion phase, the following can be stated. At early part of combustion, flame topology is similar to fuel jet one and it corresponds reasonably well with Dec's model [23] of DI diesel combustion. Later on, the flame structure becomes much more complex due to interaction with in-cylinder large-scale vortices (swirl, squish) and in this particular case, there is also interaction with walls of piston bowl. All of that is magnified by strong in-cylinder turbulent diffusion. Hence, burning zone is located near outer walls of piston bowl and it does not follow fuel jet topology any more. Local flame temperatures are within expected range while peak values are approx. 2700-2800 K, which is consistent with [23].

Finally, CCV effects are touched. Only single-cycle CFD calculations are shown in this paper while the measured/reference data correspond to average cycle. Multi-cycle simulations are planned for the near future. However, it is expected that these multi-cycle results will not differ significantly (from single-cycle ones) due to the well-known fact that CCV levels are low in CI ICEs. Hence, the results/conclusions presented in this paper are expected to be valid without taking CCV effects into account.

ACKNOWLEDGEMENTS

LIST OF NOTATIONS AND ABBREVIATIONS

CCV	Cycle-to-Cycle Variation(s)
CFD	Computational Fluid Dynamics
CI	Compression Ignition
COV	Coefficient of Variation
DDM	Discrete Droplet Method
DI	Direct Injection
EGR	Exhaust Gas Recirculation
HP	High Pressure
IMEP	Indicated Mean Effective Pressure
ICE	Internal Combustion Engine
IVC	Intake Valve Closing
KE	Kinetic Energy
LES	Large Eddy Simulation
PDF	Probability Density Function
PM	Particulate Matter
ROHR	Rate of Heat Release
SI	Spark Ignition
SW	Software
RANS	Reynolds Averaged Navier-Stokes (equation set)
TKE	Turbulence Kinetic Energy

REFERENCES

[1] Vitek, O., Macek, J., Tatschl, R., Pavlovic, Z. et al., LES Simulation of Direct Injection SI-Engine In-Cylinder Flow, SAE Technical Paper 2012-01-0138, 2012, doi.org/10.4271/2012-01-0138

[2] Tatschl, R., Bogensperger, M., Pavlovic, Z., Priesching, P. et al., LES Simulation of Flame Propagation in a Direct-Injection SI-Engine to Identify the Causes of Cycle-to-Cycle Combustion Variations, SAE Technical Paper 2013-01-1084, 2013, doi.org/10.4271/2013-01-1084

[3] Vítek, O., Macek, J., Pavlovic, Z., et al., Statistical Analysis of Detailed 3-D CFD LES Simulations with Regard to CCV Modeling, Journal of Middle European Construction and Design of Cars, 14(1), pp. 1-16, 2016. doi:10.1515/mecdc-2016-0001

[4] Richard S., Colin O., Vermorel O., Benkenida A., Angelberger C. and Veynante D., Towards Large Eddy Simulation of Combustion in Spark Ignition Engines, Proceedings of the Combustion Institute, Vol. 31, No. 1, pp. 3059-3066, 2007.

[5] Moureau, V., Barton, I., Angelberger, C., Poinsot, T., Towards Large Eddy Simulation in Internal-Combustion Engines: Simulation of a Compressed Tumble Flow, SAE Technical Paper 2004-01-1995, 2004. doi: 10.4271/2004-01-1995

[6] Vermorel, O., Richard, S., Colin, O., Angelberger, C., Benkenida, A., Veynante, D., Multi-Cycle LES Simulations of Flow and Combustion in a PFI SI 4-Valve Production Engine, SAE Technical Paper 2007-01-0151, 2011. doi: 10.4271/2007-01-0151

[7] Pera, C., Angelberger, C., Large Eddy Simulation of a Motored Single-Cylinder Engine Using System Simulation to Define Boundary Conditions: Methodology and Validation, SAE Int. J. Engines 4(1):948-963, 2011. doi: 10.4271/2011-01-0834

[8] Thobois, L., Rymer, G., Soulères, T., Poinsot, T., Large Eddy Simulation in IC Engine Geometries, SAE Technical Paper 2004-01-1854, 2004. doi:10.4271/2004-01-1854

[9] Hori, T., Kuge, T., Senda, J., and Fujimoto, H., Large Eddy Simulation of Diesel Spray Combustion with Eddy-Dissipation Model and CIP Method by Use of KIVALES, SAE Technical Paper 2007-01-0247, 2007. doi.org/10.4271/2007-01-0247

[10] Banerjee, S., Liang, T., Rutland C. J., and Hu, B., Validation of an LES Multi Mode Combustion Model for Diesel Combustion, SAE Technical Paper 2010-01-0361, 2010. doi.org/10.4271/2010-01-0361

[11] Mobasheri, R., and Peng, Z., Using Large Eddy Simulation for Studying Mixture Formation and Combustion Process in a DI Diesel Engine, SAE Technical Paper 2012-01-1716, 2012. doi.org/10.4271/2012-01-1716

[12] Wang, Z., Swantek, A., Scarcelli, R., Duke, D. et al., LES of Diesel and Gasoline Sprays with Validation against X-Ray Radiography Data, SAE Int. J. Fuels Lubr. 8(1):147-159, 2015. doi.org/10.4271/2015-01-093

[13] Farrace, D., Panier, R., Schmitt, M., Boulouchos, K. et al., Analysis of Averaging Methods for Large Eddy Simulations of Diesel Sprays, SAE Int. J. Fuels Lubr. 8(3):568-580, 2015. doi.org/10.4271/2015-24-2464

[14] Blomberg, C., Zeugin, L., Pandurangi, S., Bolla, M. et al., Modeling Split Injections of ECN "Spray A" Using a Conditional Moment Closure Combustion Model with RANS and LES, SAE Int. J. Engines 9(4):2107-2119, 2016. doi.org/10.4271/2016-01-2237

[15] R. I. Issa, Solution of the Implicitly Discretized Fluid Flow Equations by Operator-splitting, In Journal of Computational Physics, Volume 62, Issue 1, 1986, Pages 40-65, ISSN 0021-9991. doi.org/10.1016/0021-9991(86)90099-9

[16] Lesieur, M., Métais, O., Comte, P. Large-Eddy Simulations of Turbulence, Cambridge: Cambridge University Press, 2005. doi:10.1017/CBO9780511755507.

[17] Smagorinsky, J., General Circulation Experiments with the Primitive Equations, Mon. Weather Rev., Vol. 91(3): 99-164, 1963.

[18] Hiromichi Kobayashi, The Subgrid-scale Models Based on Coherent Structures for Rotating Homogeneous Turbulence and Turbulent Channel Flow, Physics of Fluids, 17, 045104, 2005.

[19] Hiromichi Kobayashi, Hama, F. and Wu, X., Application of a Local SGS Model Based on Coherent Structures to Complex Geometries, International Journal of Heat and Fluid Flow 29 (2008) 640-653.

[20] Zeldovich, Y. B., Sadovnikov, P. Y. and Frank-Kamenetskii, D. A., Oxidation of Nitrogen in Combustion, Translation by M. Shelef, Academy of Sciences of USSR, Institute of Chemical Physics, Moscow-Leningrad, 1947.

[21] Dukowicz, J.K., A Particle-Fluid Numerical Model for Liquid Sprays, J. Comp. Physics, 35, 229-253, 1980.

[22] Heywood, J. B., Internal Combustion Engine Fundamentals, McGraw-Hill series in mechanical

engineering, printed in USA. McGraw-Hill, 1988. ISBN 0-07-028637-X.

[23] Dec, J. E., A Conceptual Model of DI Diesel Combustion Based on Laser-Sheet Imaging, Technical Paper 970873, 1997. doi.org/10.4271/970873

[24] Lovas, T., Mauss, F., Hasse C. and Peters, N., Modeling of HCCI Combustion Using adaptive Chemical Kinetics, SAE Technical Paper 2002-01-0426, 2002.

[25] Kong, S.C., Marriott, C.D:, Reitz, R.D. and Christensen, M., Modeling and Experiments of HCCI Engine Combustion Using Detailed Chemical Kinetics with Multidimensional CFD, SAE 2001-01-1026, 2001.

[26] Liang L., Stevens J.G., Farell J.T., A dynamic multi-zone partitioning scheme for solving detailed chemical kinetics in reactive flow computations, Combust. Sci. and Tech. 181: 1345-1371, 2009.

[27] Vávra, J., Bortel, I., Takáts, M., Diviš, M., Emissions and performance of diesel-natural gas dual-fuel engine operated with stoichiometric mixture, Fuel, 2017 (Volume 208), p. 722-733. ISSN 0016-2361. doi.org/10.1016/j.fuel.2017.07.057

[28] Reitz, R. D., Mechanisms of Atomization Processes in High-Pressure Vaporizing Sprays, Atomization and Spray Technology. 3. 309–337. 1987.

[29] Reitz, R. D. and Bracco, F. V., Mechanisms of Breakup of Round Liquid Jets, The Encyclopedia of Fluid Mechanics, ed. N. Cheremisnoff. 3. 223–249. 1986.

[30] Mehl M., Pitz, W. J., Westbrook, C. K., Curran, H. J., Kinetic Modeling of Gasoline Surrogate Components and Mixtures Under Engine Conditions, Proceedings of the Combustion Institute 33:193-200 (2011).

[31] Westbrook, C. K., Pitz, W. J., Herbinet, O., Curran, H. J. and Silke, E.J., A comprehensive detailed chemical kinetic reaction mechanism for combustion of n-alkane hydrocarbons from n-octane to n-hexadecane, Combustion and Flame 156:181-199 (2009).

[32] Pei, Y., Mehl, M., Liu, W., Lu, T., Pitz, W. J. and Som, S., A Multi-Component Blend as a Diesel Fuel Surrogate for Compression Ignition Engine Applications, Journal of Engineering for Gas Turbines and Power, GTP-15-1057 (2015).

[33] Smith, G. P., Golden, D. M., Frenklach, M., Moriarty, N. W., Eiteneer, B., Goldeberg, M., Bowman, C. T., Hanson, R. K., Song, S., Gardiner, W. C., Jr., Lissianski, V.V. and Qin, Z., http://www.me.berkeley.edu/gri_mech/

[34] Kyrtatos, P., Brückner, C., Boulouchos, K., Cycle-to-Cycle Variations in Diesel Engines, Applied Energy, Volume 171, 2016, Pages 120-132, ISSN 0306-2619. doi.org/10.1016/j.apenergy.2016.03.015.

[35] Torelli, R., Matusik, K., Nelli, K., Kastengren, A. et al., Evaluation of Shot-to-Shot In-Nozzle Flow Variations in a Heavy-Duty Diesel Injector Using Real Nozzle Geometry, SAE Technical Paper 2018-01-0303, 2018. doi.org/10.4271/2018-01-0303

[36] AVL AST (2017.1). FIRE Manual v2017.1, AVL List GmbH, Graz.

[37] GT-Power User's Manual, GT-Suite version 7.3. Gamma Technologies Inc., 2012.